Syndecan functions to regulate Wnt-dependent axon guidance in *C. elegans*

Samantha N. Hartin and Brian D. Ackley

Department of Molecular Biosciences, University of Kansas, Lawrence, KS

Corresponding Author:

Brian D. Ackley

5004 Haworth Hall

1200 Sunnyside Ave

Lawrence, KS 66045

bdackley@ku.edu

9 Figures, 7 Tables, 1 Supplemental Table

56 Pages

Abstract: 234 Words

Introduction: 684 Words

Results: 5335 Words

Discussion: 1715 Words

Running title: Syndecan – Wnt Axon Guidance

Abstract

Syndecans are conserved cell-surface receptors that function in multiple developmental contexts. We found that *C. elegans* with mutations in the single syndecan gene, *sdn-1,* exhibited errors in anterior-posterior axon growth and termination, including axons that stopped short of or grew past their stereotypical termination point. Transgenic rescue experiments indicated that syndecan function was cell non-autonomous for GABAergic axon outgrowth during early development, but likely cell autonomous to inhibit growth later in development. In regulating the posterior termination of the GABAergic motorneurons in the dorsal nerve cord, *sdn-1* appeared to function to regulate the inhibitory activity of the *egl-20/Wnt* ligand. Over-expression of EGL-20 induced premature axon termination, and this was enhanced by loss of *sdn-1.* Conversely, removing *egl-20* from *sdn-1* mutants resulted in fewer animals with prematurely terminating dorsal nerve cords. The proteoglycan modifying enzymes *hse-5* and *hst-2*, but not *hst-6*, had similar effects, suggesting specific heparan sulfate modifications regulated EGL-20 axon-terminating activity. *sdn-1* appears to function with *lin-17/Frizzled*, *bar-1/*β-catenin and the *egl-5* Hox-like transcription factor in EGL-20-depedent axon outgrowth. We found that *bar-1* was required for *egl-5* expression in the most posterior GABAergic neurons. *sdn-1* mutants had a more variable effect on *egl-5* expression, but over-expression of *egl-5* was able to partially rescue phenotypes caused by the loss of *sdn-1.* Overall our results suggest that syndecan is a component of a specific Wnt-signaling event that is necessary for axons to recognize appropriate termination points.

Introduction

The development of the nervous system is a highly ordered and complex process that relies on axons interpreting multiple molecular cues to form functional circuits. During development axonal growth cones are guided by signals in the extracellular matrix (ECM) to their correct position. *Caenorhabditis elegans* provides a valuable model in which to study nervous system development. In particular, the growth and termination of the GABAergic motorneurons have proven useful in identifying novel axon guidance factors and/or new roles for known guidance cues (Hobert et al., 1999; Huang et al., 2002; Huang et al., 2003; Huarcaya Najarro and Ackley, 2013; Opperman and Grill, 2014; Wightman et al., 1997).

Heparan sulfate proteoglycans and chondroitin sulfate proteoglycans (HSPGs and CSPGs, respectively) modulate signals that are crucial for proper axon guidance (Bulow et al., 2008; Diaz-Balzac et al., 2014; Lee and Chien, 2004; Rawson et al., 2005; Rhiner et al., 2005; Shen, 2014; Yamaguchi, 2001). HSPGs and CSPGs can be secreted into the ECM, or be transmembrane-associated proteins on the cell surface. The core of these proteins are decorated with heparan sulfate (HS) and chondroitin sulfate (CS) side chains (Bernfield et al., 1992; Diaz-Balzac et al., 2014; Lee and Chien, 2004). The individual sugars on these side chains are enzymatically modified, e.g. by epimerases and sulfotransferases, to alter protein function (Bulow and Hobert, 2004; Wang et al., 2015). For example, the HS- or CS-side chains can regulate the binding affinity and avidity for multiple signaling molecules including Wnts, FGFs and BMPs. As a functional consequence of these modifications, HSPGs and CSPGs can modulate growth factor signaling in multiple ways, *e.g.* creating growth factor reservoirs in the ECM or functioning as co-

receptors on the cell surface (Aricescu et al., 2002; Baeg and Perrimon, 2000; Bishop et al., 2007; Inatani et al., 2003; Steigemann et al., 2004; Tumova et al., 2000; Yamaguchi, 2001).

Syndecans comprise one of the major families of HSPGs. Syndecan HSPGs not only have HS side chains but the intracellular domain can contain a PDZ-domain binding motif suggesting that syndecans can may link to cytoplasmic signaling via PDZ-domain containing proteins (Cohen et al., 1998; Hsueh and Sheng, 1999). Most mammalian genomes encode for four syndecan proteins, while the *C. elegans* genome encodes only one, named *sdn-1*. In *C. elegans*, SDN-1 functions autonomously in the Hermaphrodite Specific Neurons (HSNs) to control cell migration and axon outgrowth and in Dorsal D-type and Ventral D-type motorneurons (DDs and VDs, respectively) to guide commissure growth along the dorsal-ventral axis (Rhiner et al., 2005). SDN-1 has also been shown to regulate the guidance of non-neural tissues including the distal tip cells (DTC) that migrate along the anterior-posterior axis to form the gonad during larval development.

Syndecan has been implicated in Wnt signaling in vertebrates and invertebrates alike (Alexander et al., 2000; Dejima et al., 2014; Schwabiuk et al., 2009). In *C. elegans* DTC guidance by SDN-1 interacts with the Wnt ligand, EGL-20. In early embryogenesis SDN-1 functions in a MOM-2/Wnt-dependent signaling event to direct cell specification (Dejima et al., 2014). We have previously demonstrated that SDN-1 and LIN-44 function in genetically-redundant pathways during gastrulation. Together these data indicate that SDN-1 is likely to function in multiple Wnt growth factor signaling events.

Here we have found evidence of SDN-1 function with another *C. elegans* Wnt ligand, EGL-20, in an antagonistic fashion, to control the precise termination of GABAergic motor neurons within the dorsal nerve cord along the anteroposterior body axis. Rescue experiments suggest the effects of SDN-1 on

axon termination were both cell-autonomous and non-autonomous. Additional epistasis experiments suggested that *sdn-1* acted genetically downstream of EGL-20/Wnt, with the LIN-17/Frizzled, and upstream of the MIG-5/Dishevelled, BAR-1/β-catenin and EGL-5/Hox transcription factor. Similar types of results have previously been demonstrated in Wnt signaling for the CAM-1/Ror tyrosine kinase (Forrester et al., 1999; Forrester et al., 2004; Green et al., 2007; Hayashi et al., 2009; Kennerdell et al., 2009; Minami et al., 2010; Ohama and Hayashi, 2009; Song et al., 2010). Our results suggest that SDN-1 modulates Wnt signaling to facilitate axon outgrowth early in development, and subsequently to be allometric with organismal growth as development progresses.

Materials and Methods

Strains and Genetics

N2 (var. Bristol) was used as the wild-type reference strain in all experiments. Strains were maintained at 18-22 ºC, using standard maintenance techniques as described (Brenner, 1974). Alleles used in this report include: *LGI, lin-44(n1792), lin-44(gk360814), lin-17(n671); LGII, mig-5(rh94); LGIII, egl-5(n945); LGIV, egl-20(lq42), egl-20(gk453010); LGV, mom-2(or77); LGX bar-1(ga80), sdn-1(ok449), sdn-1(zh20), hse-5(tm472), hse-5(lq49), hst-2(ok595), hst-6(ok273).* The following integrated transgenic lines were used: *lhIs47* [*Punc-25::mCherry*], *juIs76* [*Punc-25::gfp*], *oxIs12 [Punc-47::gfp], muIs32* [*Pmec-7::gfp*], *juSi119* [*Psdn-1::SDN-1cDNA::GFP::sdn-1 3'UTR*] (Dejima et al., 2014), *wpSi12* (Edwards and Hammarlund, 2014), *lqIs80* [*Pscm::gfp*], *wpIs54* [*Pegl-5::EGL-5::GFP-3xFLAG*] (Niu et al., 2011). The following transgenic arrays were used: *lhEx435* [*Punc-25::mCherry* - 5 ng/µl], *lhEx457, lhEx458* [*Plin-17::lin-17::rfp* - 2 ng/µl], *lhEx350, lhEx353, lhEx354,* [*Pegl-20::egl-20::gfp* - 5 ng/µl], *lhEx512* [*Pmig-5::mig-5::gfp* - 2 ng/µl]; *lhEx495* [*Punc-25::sdn-1* - 1 ng/µl]; *lhEx492, lhEx493* [*Punc-25::sdn-1* - 5 ng/µl]; *lhEx523* [*Punc-25::sdn-1::gfp* - 1 ng/µl].

Plasmid Construction

A *sdn-1* cDNA was obtained from a cDNA library, initially transcribed by random hexamers and Superscript III (Life Technologies). The primers used to amplify the cDNA were as follows: *sdn-1cDNAF1* 5' – caggtgattacaccaacaagac – 3' and *sdn-1cDNA R1* 5'- cagataagtgccatcagaaacc – 3'. The resulting PCR product was cloned into the pCR8/GW/Topo entry vector (Life Technologies) to make pEVL424, and then recombined into the *Punc-25* destination vector (pBA153) using LR recombinase (Life Technologies) per the manufacterer's protocol to generate pEVL449. The *sdn-1* cDNA was sequenced prior to recombination to ensure no errors were created by

PCR. To generate pEVL454 (P*unc-25::sdn-1::gfp*) we cut pEVL424 with *BstBI,* and ligated in the gfp cassette from pPD113.37 (a gift of A. Fire) with *ClaI.* Any additional cloning details are fully available upon request.

Fluorescence microscopy

Axon termination (GABAergic neurons) was visualized using *juIs76, oxIs12, lhIs47* or *lhEx435* or (mechanosensory neurons) *muIs32*. Scoring and imaging were done using an Olympus FV1000 confocal microscope. Animals where the DNC bundle did not grow to the posterior edge the cell bodies located on the VNC, were considered under-extended. Animals in which the DNC axons grew past the cell bodies located on the VNC, were considered to be over-extended. In cases where the VD motorneuron cell bodies were displaced the position of the anus was used as a secondary landmark. Animals with posterior neurites (PNs) or other obvious axon guidance errors during commissural growth were not included in the analysis of DNC termination points.

Statistics

A Fisher's exact test was used to evaluate the statistical significance between genotype pairs. P values were calculated with Prism GraphPad (5.0) program or the GraphPad QuickCalcs (http://www.graphpad.com/quickcalcs/). A multiple test correction (Bonferroni) was applied when used to evaluate relationships within groups of genotypes, relative to the number of comparisons being made within that experimental design. For example, we considered a significant effect to be <0.05 for pairwise comparisons, and <0.017 for three-way comparisons, etc.

Results

Syndecan is an anterior/posterior axon guidance factor

The GABAergic D-type motorneurons cell bodies are located along the ventral nerve cord (VNC). The six Dorsal D-type (DD) and thirteen Ventral D-type (VD) cell bodies extend a single neuronal process anteriorly. The axon stalls, and initiates a dorsal commissural process and then a second process initiates from the stall point and extends a second anterior branch to the next most anterior VD neuron (Figure 1) (Huarcaya Najarro and Ackley, 2013). The commissural process upon reaching the dorsal nerve cord (DNC) bifurcates and sends processes both anteriorly and posteriorly. In the VNC and DNC, the DD processes fasciculate with those of the VD neurons and terminate at stereotyped positions along the anteroposterior axis (White et al., 1986). The most posterior DD and VD processes extend as a bundle that terminates at the anteroposterior position superior to the locations of the DD6 and VD13 cell bodies, which are located on the ventral side (Maro et al., 2009) (Figure 1A and B). The stereotyped development allows for easy detection of aberrant axon patterning phenotypes.

We observed that *sdn-1(zh20)* mutants had defects in formation of the GABAergic motorneurons along the anterior-posterior (A-P) axis of the animal. Animals with mutations in the *sdn-1* exhibited posterior neurites (PNs) (16%±7), where an axonal process was inappropriately projected toward the posterior of the animal (Huarcaya Najarro and Ackley, 2013). In animals where the axon projected normally toward the anterior we also observed defects in where axons terminated along the A-P axis in the dorsal nerve cord (Figure 1). We found that 35%±13 of *sdn-1(zh20)* mutants had axons that stopped short of the stereotyped termination point, while 26%±10 had axons that extended posteriorly past the proper termination point (Figure 1 D-F, Table 1). It is worth noting that in other genetic contexts where

D-axon termination has been investigated it is common to observe both under- and over-extension defects in the same genotypes (Maro et al., 2009; Opperman and Grill, 2014).

We also tested a second LOF allele, *sdn-1(ok449)* which results in an in-frame deletion that produces a shortened form of SDN-1. This shortened form lacks two of the major conserved heparan sulfate attachment sites in the extracellular domain (Minniti et al., 2004). We found that animals with the *ok449* mutation had similar defects to those found with the *zh20* allele. We continued our studies using the *zh20* allele since that has been demonstrated to be a genetic and molecular null (Rhiner et al., 2005, Dejima et al., 2014).

The VD neurons are formed at the end of the first larval stage (L1) and finish their initial outgrowth during the beginning of the second larval stage (L2). We initially scored animals in the fourth larval stage (L4). Between the L2 and L4 stages the animals approximately double in length. During development the posterior segment of the DNC (from the point of the final commissural branch to the terminus) increases from ~25-30 μm (L2) to ~30-40 μm (L4), and continues growing to ~50-60 μm in wild-type young adults. To determine if *sdn-1* axon outgrowth errors were due to developmental errors or a failure to keep up with the growth of the animal we scored DNC termination in *zh20* animals at the L2 stage. We found that like those scored at later stages, *zh20* animals at the L2 stage had both under- (52%) and over- (27%) extended GABAergic axons in the DNC. We concluded from this analysis that, during initial formation, the DNC terminated growth prematurely in a majority of animals lacking *sdn-1* (Table 1).

To determine if the effects of axon termination along the anterior-posterior axis were limited to the D-type neurons we examined the axons of the six mechanosensory neurons using an integrated GFP reporter, *muIs32.* In wild-type animals the Anterior Lateral Mechanosensory (ALMs) and the Posterior

Lateral Mechanosensory (PLMs) neurons extend anteriorly-directed axons from their cell bodies and have a characteristic termination point, with the PLMs terminating just posterior to the ALM cell bodies (Figure 1) and the ALMs terminating just posterior to the nose of the animal. In addition, the axons are largely parallel to the dorsal and/or ventral nerve cords, and do not appear to deviate in the dorsal-ventral axis, except where they make branches into the ventral nerve cord (PLMs) or the nerve ring (ALMs).

When we examined the ALM and PLM neurons in *sdn-1(zh20)* mutant animals we found disruptions in the outgrowth of the neurons. As had been previously reported the ALM cell bodies were frequently displaced posteriorly, likely due to incomplete cell migration (Rhiner et al., 2005). Because of these cell migration defects we did not score axon termination errors in the ALMs. The PLM neurons do not undergo long range cell migrations, and were located in grossly normal positions in *zh20* mutants. We found that PLM axons that were shortened in *zh20* animals (14%±4, N=207), either by terminating prematurely or not elongating sufficiently during organismal growth. We also found instances where PLMs were over-extended, and could "hook" toward the ventral nerve cord (17%±6) (Figure 1) (Grill et al., 2007). Overall these defects were less penetrant than those we observed in the DD/VD motorneurons, but were consistent with a role for *sdn-1* in regulating axon extension along the A/P axis, and that loss of *sdn-1* can result in both over- and under-growth phenotypes in different neuron types.

Syndecan function is required in multiple tissues to regulate D-type neuron outgrowth

We were able to partially rescue the outgrowth phenotypes in the D-type neurons in *sdn-1(zh20)* animals by reintroducing *sdn-1* (Table 1). We obtained a Mos1-mediated single copy insertion (MosSCI),

juSi119, in which a GFP-tagged version of SDN-1 under the regulation of *sdn-1* endogenous promoter elements had been inserted on the second chromosome (LG II) (Dejima et al., 2014). The *zh20; juSi119* animals had fewer undergrown axons in the DNC (6% vs. 35% in *zh20*, P<0.0001), but had a higher rate of DNC overgrowth (59%±4) than observed in *zh20* mutants (26%, P<0.0001). To determine if this was due to the GFP insertion we obtained a second MosSCI, *wpSi12*, which is inserted in the same chromosomal position, but is not GFP tagged (Edwards and Hammarlund, 2014). We observed rescue of the under-extension phenotype (1% vs. 35% in *zh20*, P<0.0001), but again an increase in the overgrowth phenotype (38% vs 26% in *zh20*, P=0.05).

To test whether *sdn-1* could be functioning cell-autonomously we drove expression of *sdn-1* specifically in the GABAergic neurons using the *unc-25* promoter (1 ng/μl). We found that when we cell-specifically expressed *sdn-1* we were able to partially rescue the over-extension phenotype in *zh20* in two separate lines (26% - *zh20* vs. 11%, P=0.0035 and 10%, P=0.005). In both transgenic lines the rate of under-extended axons was not significantly changed (35% - *zh20* vs. 37%, P=0.60 and 33%, P=0.91). We generated lines at a higher concentration (5 ng/μl) and found no obvious difference. We were still unable to rescue the under-extension defects (36% vs 34%, P=0.94) and there was not a robust increase in the efficiency of rescuing the over-extension defects (26% vs. 8%, P=0.002). These data suggest that the over-extension of axons in *zh20* animals was due to, at least in part, to the cell-autonomous loss of *sdn-1*, but the under-extension phenotype demonstrated a requirement for *sdn-1* function in other tissues.

Table 1. GABAergic DNC termination defects in Syndecan mutants

	% Observed (Mean ± St. Dev)				Comparison to *sdn-1(zh20)*	
	Under	WT	Over	N	P (under)	P (over)
sdn-1(zh20)	35 ± 13	39 ± 10	26 ± 10	246		
sdn-1(zh20); juSi119	6 ± 1	36 ± 3	59 ± 4	200	<0.0001 ‡	<0.0001 ‡
sdn-1(zh20); wpSi12	1 ± 1	61 ± 8	38 ± 9	216	<0.0001 ‡	0.0538

sdn-1(zh20); Punc-25::sdn-1 (A)	37 ± 13	52 ± 8	11 ± 6	81	0.6038	0.0035 ‡
sdn-1(zh20); Punc-25::sdn-1 (B)	33 ± 3	57 ± 6	10 ± 3	141	1	0.005
sdn-1(zh20); Punc-25::sdn-1::gfp	33 ± 4	67 ± 4	0 ± 0	104	1	0.005

‡ Significantly different (P< 0.005)

Syndecan is enriched in the DNC near the VD13 termination point

We examined the localization of SDN-1GFP expressed by *juSi119.* The protein was present broadly throughout the animal. We observed robust expression in the DNC and tissues surrounding it, including the muscle, epidermis and intestinal cells (Figure 2). We further examined whether SDN-1 was expressed in the D-type neurons using a cytoplasmic RFP (*Punc-25::mCherry*). We found that, while SDN-1GFP was present in the ventral and dorsal nerve cords, we were unable to detect expression in the D-type neurons. We examined animals specifically when the VD13 commissure was being formed, and found no detectable SDN-1::GFP in the growth cone (Figure 2). This was curious since previous work has suggested the *sdn-1* promoter is active in the D-type neurons (Rhiner et al., 2005). Since we were unable to rescue the overgrowth phenotype with the MosSci integrated transgenes, but we could with cell-autonomous expression could, we inferred the SDN-1 transgenes, MosSCI integrated into LGII, may have been poorly expressed in the GABAergic neurons.

While we did not detect abundant SDN-1GFP in VD neurons, we did find that, in the DNC, SDN-1GFP was enriched near the normal termination point of the GABAergic neurons (Figure 2). The VD neurons form during the L1 larval stage, in an anterior-posterior fashion, that is VD1 forms first and VD13 forms last, near the L1-L2 molt. In L1 animals, prior to the formation of the VD13, we found that SDN-1::GFP was accumulated in the nervous system, and an aggregation was present near the termination point of the DD GABAergic neurons in the DNC (Figure 2). This suggests that SDN-1::GFP is in a position to assist

the VD13 axon in identifying the proper termination point. When we examined the SDN-1::GFP after all of the VD axons had formed (Figure 2) we found that SDN-1::GFP was maintained at the termination point VD13 axon, being present in L4 (Figure 2) and adult animals (not shown).

We also generated a gfp-tagged version of SDN-1 to express specifically in the D-type neurons. The *Punc-25::*SDN-1::GFP transgene was capable of rescuing the dorsal cord growth defects as efficiently as the non-tagged version (Table 1). In these animals we observed SDN-1 in cell bodies and along the ventral, commissural and dorsal processes of the neurons (Figure 2), but no specific enrichment at the termination point of the DNC. From this analysis we concluded that SDN-1 was localized such that it could make a local contribution to GABAergic axon termination in the dorsal nerve cord, and that, within the GABAergic neurons SDN-1 could localize to the dorsal cord. We also concluded that SDN-1 accumulation near the termination point of the dorsal nerve cord likely represented contributions from multiple tissue types.

SDN-1 function is epistatic to LIN-44 in VD neurons, but not PLMs

Previous work has demonstrated that Wnt signaling can regulate axon termination of the D-type neurons (Maro et al., 2009). Consistent with those observations we also found that animals with mutations in the most posteriorly expressed Wnt ligand, *lin-44(n1792)*, caused the DNC axons to over-extend in 91%±5 of animals (Figure 3, Table 2). Previously we described that *sdn-1* and *lin-44* exhibit a synthetic lethal genetic interaction in early development, with ~75% of double mutants dying during embryogenesis (Hartin et al., 2015). To determine whether *sdn-1* was functioning in *lin-44* dependent outgrowth we generated double mutants. We were able to score the axons in the surviving animals, and

found that, unlike the *lin-44* single mutants, the doubles exhibited both under and over-extended DNCs (Figure 3, Table 2). Qualitatively, we assessed the over-extended DNCs in the *sdn-1; lin-44* mutants to be more like those of the *lin-44* animals, as they extended further into the posterior than was typically seen in *sdn-1* mutants. Thus, we concluded that *sdn-1* loss of function was partially epistatic to axon overgrowth caused by *lin-44.* Most likely, the undergrown axons terminate prior to reaching the position where they would be sensitive to the presence (or absence) of *lin-44.* However, axons that did extend past the normal termination point were affected by the loss of *lin-44* could protrude into more posterior regions of the animal.

Mutations in *lin-44* also affect the direction and extent of axon outgrowth of the PLM axons (Hilliard and Bargmann, 2006) (S. Figure 1). Loss of function in *lin-44* results in PLMs with posteriorly directed axons (54%±18, N=181) and altered lengths of posterior and anterior processes, including animals where the processes appeared to be of equal length (20%±15) and animals with longer anterior processes, but that stop short of the normal termination point (9%±4). We generated double mutants with *sdn-1* and found that the surviving *lin-44; sdn-1* animals had an increase in the number of reversed PLMs (85%±6, N=200 P<0.0001 vs *lin-44* alone). Thus, we concluded that *sdn-1* function was not epistatic to *lin-44* in PLMs, rather, in parallel. And that *sdn-1* had a similar, but weaker effect on PLM polarity as *lin-44,* but the effect was only obvious in the animals also lacking *lin-44.* To better understand how *sdn-1* functioned in axon outgrowth we focused the remainder of our study on dorsal nerve cord termination in the D-type neurons.

EGL-20 and LIN-44 function in parallel in GABAergic development

A second Wnt ligand, *egl-20,* has also been found to affect DNC termination (Maro et al., 2009). We obtained two putative null alleles of *egl-20*, *lq42* (pers. comm. Erik A Lundquist) and *gk453010* from the Million Mutation Project (Thompson et al., 2013). Both *lq42* and *gk453010* introduce premature stop codons in the *egl-20* mRNA, unlike the reference allele, *n585*, which is a missense mutation. We found that in both *egl-20(lq42)* and *egl-20(gk453010)* axons over-extended into the posterior (Table 2). Qualitatively, we observed that the extent to which the axons extended past the expected termination point was shorter in *egl-20* than in *lin-44* mutants, which is consistent with their patterns of expression, with *egl-20* being expressed in a region just anterior to the expression of *lin-44*.

We generated *lin-44; egl-20* double mutants, and found that an exceptionally high number of animals exhibited PN defects (64%±24, compared to 0.5% - *egl-20,* and 1.5% - *lin-44*), as well as additional guidance defects during commissural growth, making it difficult to accurately assess the DNC phenotype. In the small number of axons that could be scored, we found evidence of both under- and over-extended DNCs (Table 2). Qualitatively, as in the *sdn-1; lin-44* doubles, the length of the over-extended DNCs appeared more severe in the Wnt double mutant than in *sdn-1* single mutants, which is consistent with previous reports, using other alleles of *egl-20* (Maro et al., 2009). We also generated *lin-44; egl-20; sdn-1* triple mutants, which were similar to the *lin-44; egl-20* doubles, exhibiting a high rate of PN defects, as well as over- and under-extended DNCs.

These results suggest there are multiple Wnt-mediated events in the development of the GABAergic neurons where EGL-20 and LIN-44 were functioning. First, EGL-20 and LIN-44 functioned redundantly to instruct growth anteriorly from the cell body. Subsequently, EGL-20 and LIN-44 functioned in a partially

overlapping manner to regulate guidance of the axons including the where the axons would terminate in the DNC.

Table 2. Wnt ligands and *sdn-1* DNC termination phenotypes

	% Observed (Mean ± St. Dev)				Comparison to *sdn-1*		PN %	N
	Under	WT	Over	N	P (under)	P (over)		
lin-44	1 ± 1	8 ± 3	91 ± 5	197			2 ± 2	200
lin-44; sdn-1	27 ± 6	35 ± 11	38 ± 10	118	0.2247	0.0026 ‡	16 ± 1	140
egl-20	0 ± 0	29 ± 4	71 ± 4	176			0 ± 1	177
egl-20; sdn-1	15 ± 4	39 ± 18	45 ± 15	224	<0.0001 ‡ * (<0.0001 ‡ *)	0.0007 ‡ (<0.0001 *)	22 ± 16	291
lin-44; egl-20	12 ± 10	12 ± 2	76 ± 13	78	Comparison to *lin-44; egl-20*		64 ± 24	252
lin-44; egl-20; sdn-1	15 ± 12	9 ± 5	76 ± 7	74	0.8066	0.523	69 ± 7	236

‡ Significantly different (P< 0.005)

** Significantly different from egl-20 (P< 0.005)*

SDN-1 inhibits EGL-20 axon repulsion during early DNC formation

We next examined *sdn-1; egl-20* double mutants. We found a reduction in the penetrance of the under-extension phenotype present in animals lacking both *egl-20* and *sdn-1* (Table 2). One interpretation of this was that, in *sdn-1* mutants, EGL-20 was inducing premature termination of the DNC. Previous results have found that EGL-20 diffusion is regulated by SDN-1 (Schwabiuk et al., 2009), and this would be consistent with EGL-20 exerting an inhibitory effect with a longer range of action when SDN-1 was absent. We tested this by expressing an EGL-20::GFP from its endogenous promoter. We found that the axons normally terminated near the site where the EGL-20::GFP protein accumulated (Figure 4). Further, we found that over-expression of EGL-20 induced under-extension phenotypes in otherwise wild-type animals (Figure 5). We crossed the transgene with the lowest rate of under-extension defects (*lhEx350)* into animals lacking *sdn-1.* The penetrance of under-extension defects increased from 9% to 63%(±10%), which was significantly higher than expected for animals simply lacking

sdn-1 (P<0.0001). These results indicate that over-expression of EGL-20 could induce premature termination of the GABAergic neurons in a syndecan-dependent manner.

We reasoned that, perhaps, the increased over-extension defects we observed in the integrated SDN-1 lines could also be due to the transgene interfering with normal EGL-20 activity. We reduced the amount of SDN-1 being produced by making the inserted *juSi119* transgene heterozygous (Figure 5). In those animals the over-extension phenotype was reduced from 59% to 21%, suggesting it was possible that the over-extension observed was due to the amount of SDN-1 being produced. We ectopically expressed *sdn-1* in the musculature, using the *myo-3* promoter, which induced over-extension defects (43%) in otherwise wild-type animals. Genetically removing *sdn-1* from these animals reduced the over-extension to (9%). Finally, we examined animals expressing the SDN-1::GFP in the GABAergic neurons. In otherwise wild-type animals this was also able to induce over-extension of the DNC. Ultimately we concluded that over-expression of SDN-1 could result in GABAergic neurons over-extending into the posterior of the animal, in a concentration-dependent manner, but independent of the source of SDN-1 being produced.

HS modifiers interact with LIN-44 and EGL-20 in a context-dependent manner

Interactions between Wnt ligands and HSPGs are often mediated by the side chains present on the core protein. It has been demonstrated that the glycosaminoglycan side chains on SDN-1 are modified by an epimerase, HSE-5, and at least two sulfotransferases, HST-2 and HST-6 (Bernfield et al., 1992; Lee and Chien, 2004). Each enzyme has been shown to be involved in multiple aspects of neural development through the specific modifications each makes (Bulow and Hobert, 2004; Bulow et al., 2008; Diaz-Balzac

et al., 2014; Rhiner et al., 2005). We examined the loss of function mutation for the three modifying enzymes to determine whether heparan sulfate sugar modifications are important for interactions with EGL-20.

HSE-5 is a C5-epimerase that is predicted to catalyze the chain-modifying epimerization of glucuronic acid to iduronic acid during heparan sulfate biosynthesis. HSE-5 is predominantly expressed in the hypodermis and intestine (Bulow and Hobert, 2004). Previously, HSE-5 has been shown to function in parallel to SDN-1 for D-type motorneuron dorsally-directed commissure outgrowth and VNC fasciculation (Rhiner et al., 2005). Animals with loss of function in *hse-5* exhibited both under- and over-extension phenotypes in the DNC (Table 3), indicating that the activity of this enzyme does contribute to anterior/posterior outgrowth of D-type axons. Double mutants of *hse-5* and *sdn-1* had an additive effect, inducing under-extension defects in 77%±3 animals, consistent with the genes functioning in parallel.

We subsequently asked whether loss of *hse-5* affected the penetrance of defects in EGL-20-dependent outgrowth (Table 3). The *egl-20; hse-5* double mutants had fewer under-extended DNCs (4% vs. 45% - *hse-5*, P<0.001), consistent with EGL-20 inducing premature termination in animals lacking HSE-5 activity. The double mutants were not significantly different for over-extended DNCs from *egl-20* single mutants (Table 3), suggesting the loss of *hse-5* was not further affecting this phenotype.

HST-2 and HST-6 can add sulfate moieties to side chains after epimerization by HSE-5. During neuronal development *hst-6* is expressed in neuronal tissues and *hst-2* is expressed in the hypodermis (Bulow and Hobert, 2004). We observed a lower penetrance of under-extension defects in *hst-2* (23%) and *hst-6* (13%) mutants compared to either *hse-5* or *sdn-1* mutants. However, like *hse-5* and *sdn-1,* we found that removing *egl-20* resulted in a reduction in the penetrance of under-extension defects

mutants in the transferase mutants (Table 3). Overall, we concluded that loss of function in the modifier enzymes were similar, but not equivalent to the loss of SDN-1, consistent with other reports examining the contributions of the core protein and modifiers to proteoglycan functions (Dejima et al., 2014; Schwieterman et al., 2016).

Table 3. DNC phenotypes in heparan sulfate modifying enzyme genes

	% Observed (Mean ± St. Dev)				Comparison to *HS* single mutant	
	Under	WT	Over	N	P (under)	P (over)
hse-5	45 ± 2	29 ± 2	27 ± 4	250		
hse-5; sdn-1	77 ± 3	17 ± 8	6 ± 5	201	<0.0001 ‡	<0.0001 ‡
hse-5; egl-20	4 ± 5	28 ± 4	69 ± 9	112	<0.0001 ‡	<0.0001 ‡
hst-2	17 ± 8	41 ± 15	42 ± 6	127		
hst-2; egl-20	8 ± 12	34 ± 10	58 ± 1	217	0.2366	0.0251
hst-6	11 ± 3	48 ± 23	41 ± 20	137		
hst-6; egl-20	2 ± 2	34 ± 13	64 ± 11	246	0.0013 ‡	0.0012 ‡

‡ *Significantly different (P<0.0063)*

sdn-1 **functions in a canonical Wnt signaling pathway to promote axon extension**

Wnt signaling in *C. elegans* has been well characterized, and in a canonical signaling pathway, activation of Frizzled receptors by Wnt ligands activates the cytosolic protein Dishevelled to inhibit the GSK3/Axin/APC complex, allowing β-catenin to activate the transcription of target genes with the help of TCF-LEF transcription factors (Buechling and Boutros, 2011). If EGL-20 were simply activating the canonical signaling pathway, then we would expect loss of function in downstream components to mimic the loss of *egl-20.* Instead, consistent with previous reports, we found Wnt signaling mutants had both under- and over-extension defects in the DNC (Table 4). Mutations in *lin-17/*Frizzled (26%±2), *dsh-1/*Dishevelled (28%±0) or *mig-5/*Dishevelled (55%±2) each resulted in under-extension of the DNC, similar to data previously reported (Maro et al., 2009).

We created double mutants of *sdn-1* with the above Wnt signaling genes. We found that removal of *lin-17* did not grossly change the outcomes for DNC phenotypes from *sdn-1* or *lin-17* single mutants (Table 4), suggesting they were functioning in a common genetic pathway. Consistent with this we found that removing *egl-20* from *lin-17* resulted a reduction in the under-extension phenotype (Table 4), as it had when we removed *egl-20* from *sdn-1* mutants. For Dishevelled, removing *sdn-1* from the *dsh-1* mutants resulted in an additive effect that was significantly different from either single mutant (Table 4). The double mutants of *sdn-1* and *mig-5* were nearly synthetic lethal, with only a very small percent (~10%) of the animals surviving to adulthood. In those survivors we observed under-extension, but it was not significantly different from *mig-5* alone. We concluded that *sdn-1* and *mig-5* function in parallel pathways during early development, but that during GABAergic DNC extension, they likely function in the same pathway, with *mig-5* epistatic to *sdn-1.*

Table 4. Frizzled and Disheveled DNC termination phenotypes

	% Observed (Mean ± St. Dev)				Comparison to *sdn-1*	
	Under	WT	Over	N	P (under)	P (over)
lin-17	26 ± 2	36 ± 21	38 ± 19	230		
lin-17; sdn-1	38 ± 10	30 ± 4	31 ± 6	151	0.6656	0.0812
lin-17; egl-20	4 ± 2	11 ± 6	85 ± 5	165	0.0188 *	0.0028 ‡*
dsh-1	28 ± 0	65 ± 5	8 ± 5	166		
dsh-1; sdn-1	69 ± 9	28 ± 11	3 ± 2	158	<0.0001 ‡	<0.0001 ‡
mig-5	55 ± 2	24 ± 1	21 ± 3	128		
mig-5; sdn-1	58 ± 15	34 ± 12	7 ± 3	83	<0.0001 ‡	0.0104

‡ Significantly different (P<0.0063)

(* comparison to *egl-20* single)

LIN-17 co-localizes with SDN-1 during neurite outgrowth in an EGL-20-dependent manner

Our results suggested that LIN-17 was functioning in a manner largely equivalent to SDN-1. To determine if LIN-17 was localized to the DNC we expressed a full-length rescuing LIN-17::tagRFP chimera,

under the control of the endogenous promoter (Figure 6) (Huarcaya Najarro and Ackley, 2013). LIN-17::RFP was prevalent throughout the animal, including the posterior region of the dorsal nerve cord and surrounding tissues. We examined the localization of LIN-17::RFP relative to SDN-1::GFP in the *juSi119* animals. We found an equivalent enrichment of LIN-17 and SDN-1 at the termination point of the DNC in wild-type animals.

Previous work suggested that LIN-17 localization in mechanosensory neurons was dependent on EGL-20/Wnt signaling. We asked whether this was true in the DNC by crossing the LIN-17::RFP and SDN-1::GFP transgenes into *egl-20* loss-of-function animals. We found that LIN-17 was no longer enriched in the posterior branch of the most posterior D-type neuron in young (L2) animals (Figure 6). However, later in development (L4) we could observe LIN-17 in the dorsal nerve cord in *egl-20* mutants. Thus, we concluded that, with respect to localization to the region where GABAergic axons will terminate in the DNC, LIN-17 localization was *egl-20*-dependent.

SDN-1 and EGL-20 require BAR-1 function during axon outgrowth

In contrast to the Frizzled receptor and Disheveled cytoplasmic adaptor, the loss of *bar-1/*β-catenin, results in a highly penetrant under-extension phenotype (Figure 7) ((96% - our observations); (Maro et al., 2009)). Removing either *sdn-1* or *egl-20* from *bar-1* mutants had no effect on axon growth as 93% (*sdn-1; bar-1)* and 96% (*egl-20*; *bar-1)* of the double mutants exhibited an under-extension phenotype (Table 5). Since animals with EGL-20 over-expression induces premature termination of the DNC, while loss of function mutations in *egl-20* resulted in over-extension, our results suggest that EGL-20 activity

likely functioned to repress BAR-1 activity in DNC outgrowth, which is not a canonical outcome of Wnt-ligand signaling.

Table 5. *bar-1/*β-catenin DNC termination phenotypes

	% Observed (Mean ± St. Dev)				Comparison to *bar-1*	
	Under	WT	Over	N	P (under)	P (over)
bar-1	96 ± 1	4 ± 1	0 ± 0	196		
bar-1; sdn-1	98 ± 2	2 ± 2	0 ± 0	170	0.5542	1
bar-1; egl-20	89 ± 4	10 ± 6	1 ± 2	150	0.0242	0.1901

‡ *Significantly different (P<0.0125)*

MOM-2 is not required for initial DNC formation

As the *lin-44; egl-20* double mutants resulted in a modest under-extension phenotype, while 96% of *bar-1* animals were under-extended, we asked whether a third Wnt ligand, *mom-2*, could be responsible for promoting axon outgrowth. *mom-2* is expressed in the L1 stage, in the posterior of the animal near the region where the DNC is forming (Harterink et al., 2011). We examined maternally-rescued *mom-2(or77)* homozygotes and found no evidence of under-extension in the DNC, although we did see over-extension (Table 6). Unlike *egl-20; lin-44* double mutants, removing *mom-2* did not increase the rates of under-extension in the *lin-44* or *egl-20* loss-of-function. Triple mutants were sick and difficult to obtain, so we used RNAi to knockdown *mom-2* in *lin-44; egl-20* double mutants. Although *mom-2* RNAi caused a highly penetrant embryonic lethality we were able to obtain sufficient numbers of escapers to analyze the DNCs. If *mom-2* were functioning to compensate for *egl-20* and *lin-44* to promote outgrowth we would expect the escapers to have a higher rate of under-extension. In contrast we observed a decrease in the rate of under-extension in escapers. Thus, it is unlikely that MOM-2 was functioning redundantly with LIN-44 and EGL-20 to activate BAR-1 to promote axon extension from the commissural branch point to the normal termination point.

Table 6. *mom-2* DNC termination phenotypes

	% Observed (Mean ± St. Dev)			N	Comparison to *mom-2*		% PN	N
mom-2(or77) [M+]	0 ± 0	20 ± 1	80 ± 1	200			0 ± 0	200
mom-2[RNAi]	2	20	78	100			0	100
mom-2(or77) [M+]; sdn-1	12	52	36	100	<0.0001 ‡	0.0331	14	116
mom-2(or77) [M+]; lin-44	0 ± 0	11 ± 14	89 ± 14	128	1	0.0002	3 ± 5	130
mom-2(or77) [M+]; egl-20 [M+]	3 ± 2	21 ± 25	76 ± 23	242	0.0344	0.4569	1 ± 2	243
mom-2[RNAi]; lin-44; egl-20	20 ± 12	13 ± 2	67 ± 15	23	0.0025 ‡*	0.2799 *	76 ± 2	95

‡ Significantly different (P< 0.0063)

** compared to mom-2[RNAi]*

The EGL-5 Hox gene contributes to the initial DNC formation and outgrowth

Wnt signaling in *C. elegans* has been shown to function via many downstream mechanisms, including activating the transcription of Hox genes. The *egl-5* Hox gene expressed in the most posterior portion of the animal, including in the posterior D-type motorneurons, and surrounding tissues (Niu et al., 2011) (Figure 6). A loss of function mutation in *egl-5, n945,* recapitulated the *bar-1* phenotype in the D-type neurons, causing a highly penetrant under-extended phenotype (95%). We generated double mutants of *sdn-1* with *egl-5* and found that the DNCs were almost entirely under-extended (89%; P<0.001 vs. *sdn-1* and P=0.19 vs *egl-5*) (Table 7), suggesting *sdn-1* functions in a pathway that includes *egl-5.*

To determine if *egl-5* was expressed in the DD and VD motorneurons we crossed an integrated P*egl-5*::EGL-5::GFP transgene (*wgIs54*) into a reporter for the GABAergic motorneurons (*Punc-25*::mCherry). We found, as has been reported, EGL-5::GFP expression was largely restricted to the posterior region. We observed co-incident expression of EGL-5::GFP and mCherry in the three most posterior neurons, VD12-DD6-VD13, with expression strongest in DD6 and VD13 (Figure 6). We observed expression in the posterior region of L1 animals, prior to the formation of the VD13 neuron (Figure 6), and expression was visible in the nascent VD13 (Figure 6) as soon as we could observe the differentiation marker (*Punc-25*)

which occurs as the axons are initiating growth, prior to the formation of the dorsal process (Norris and Lundquist, 2011) (Figure 2). Further, expression of EGL-5 was maintained in the neurons throughout development (L4 stage – Figure 6). Thus, we concluded that EGL-5 is expressed in the neurons (DD6 and VD13) that make posterior projections that terminate axon growth without the help of a more posterior D-type neuron, and that expression is maintained throughout the period of development when D-type neuron growth must be metered.

We crossed the *wgIs54* transgene into the *bar-1(ga80)* mutants and found that expression of the *egl-5::gfp* was lost in the DD and VD neurons, but expression could be observed in other cells adjacent (Figure 6). This suggested that EGL-5 expression in the D-type neurons was *bar-1*-dependent, and that this might underlie the under-extension defects. Similar effects of Wnt signaling activating anterior vs. posterior behaviors in cells has been documented in the migration of the Q-neuroblasts, with *mab-5* necessary and sufficient for proper posterior growth (Tamayo et al., 2013), and more recently in the axon outgrowth of PLM axons (Zheng et al., 2015).

We subsequently examined whether *sdn-1* mutants also resulted in alterations in *egl-5* expression. In contrast to *bar-1,* we did not find EGL-5::GFP expression to be lost from the D-type neurons in *sdn-1* mutants, although the pattern and intensity appeared to be more variable than in wild-type animals. We did note however, the *wgIs54* transgene partially rescued under-extension and over-extension phenotypes present in the *sdn-1* loss-of-function animals (Table 6). Thus, we concluded that underextension of the DNC in *sdn-1* animals likely occurs dysregulation of *egl-5* in the GABAergic neurons*,* likely via *bar-1*, and that it is possible to partially bypass the requirement for SDN-1 in early dorsal nerve cord development by increasing the levels of EGL-5. It should be noted that this observation

is consistent with the differences observed in the *sdn-1* and *bar-1* mutants, frequency as well as the position where the axons terminated in *bar-1* mutants was more severe than in *sdn-1*, and thus we do not believe *sdn-1* mutations resulted in a complete loss of either *bar-1* or *egl-5* activity.

Table 7. *egl-5* DNC termination phenotypes

	% Observed (Mean ± St. Dev)				Comparison to *sdn-1*	
	Under	WT	Over	N	P (under)	P (over)
egl-5	90 ± 1	10 ± 1	0 ± 0	194		
sdn-1; egl-5	89 ± 3	11 ± 3	0 ± 0	205	<0.0001 ǂ	<0.0001 ǂ
wgIs54	1 ± 1	90 ± 3	9 ± 4	123		
sdn-1; wgIs54	17 ± 1	76 ± 2	7 ± 2	206	<0.0001 ǂ	<0.0001 ǂ

ǂ Significantly different (P<0.0125)

Discussion

SDN-1 functions in anterior-posterior axon outgrowth and termination

In *C. elegans*, neural development is highly stereotyped. Here we describe a role for *sdn-1,* the single *C. elegans* ortholog of the vertebrate syndecan cell-surface HSPG receptors in axon growth along the anterior-posterior axis. Animals lacking *sdn-1* have defects whereby axons initiate axon growth in the incorrect direction, or terminate growth at the wrong position, along the anterior/posterior axis. These results are consistent with other described roles for *sdn-1* in regulation of cell migration along the A/P axis (Rhiner et al., 2005; Schwabiuk et al., 2009), and with syndecans contributing to multiple stages of neural development.

sdn-1 loss-of-function resulted in a highly penetrant growth defect in the GABAergic (DD/VD) axons in the posterior region of the dorsal nerve cord, and a less penetrant effect on the axons of the posterior mechanosensory neurons (PLMs). We observed anterior-posterior outgrowth defects in the initial axon formation in *sdn-1* mutants, including the PN phenotype we have previously described (Huarcaya Najarro and Ackley, 2013). We found that the rate of initial outgrowth errors was enhanced by loss of function in Wnt ligands, suggesting the genes function in parallel pathways to insure directional outgrowth during axon formation.

In both GABAergic and mechanosensory neurons we found axons stopping short of, and growing past, their stereotyped termination point. We observed errors in the location of termination even when other aspects (initial outgrowth, dorsal/ventral guidance, *etc.*) were grossly normal. Therefore, we concluded that the termination defects were, at least partially, independent of earlier guidance errors. Neither the PLMs nor the terminal D-type neurons (DD6 and VD13) have obvious cellular landmarks that

mark where they should terminate. This is in contrast to the more anterior DD and VD neurons that terminate their posterior dorsal branch on the next DD or VD cell posterior, that is, the posterior branch of the VD11 dorsal process terminates where it meets the anterior branch of VD12, *etc*. Because of the overlap of the DD and VD axons in the dorsal nerve cord, it is not simple to determine whether *sdn-1* has a broader role in regulating the outgrowth of dorsal branches in the D-type neurons along the anterior-posterior axis of the animal, and thus we focused solely in this work on those in the posterior-most region.

SDN-1 function is both autonomous and non-autonomous

In the D-type neurons we found an early role for SDN-1 in ensuring that the posterior neurite of the dorsal nerve cord reached the proper termination point. Based on rescue experiments, SDN-1 appeared to function cell-nonautonomously, as we were able to rescue the defects by expressing SDN-1 with an *sdn-1* promoter, but not when we replaced SDN-1 specifically in the D-type neurons. We found that *sdn-1* mutants exhibited an over-growth phenotype, where the axons grew past the normal termination point. This phenotype appeared to be cell-autonomous, as we could largely rescue this phenotype by specifically replacing SDN-1 in the GABAergic neurons. Thus, we concluded that SDN-1 is necessary in the D-type neurons to prevent overgrowth, but we cannot fully rule out a role for SDN-1 in other tissues to complement the cell-autonomous function.

One result that was somewhat curious was the rescue of *sdn-1* phenotypes by the integrated transgenes with the endogenous *sdn-1* promoter. We were able to rescue the under-growth phenotype, and other *sdn-1* phenotypes, including uncoordinated movement and male mating (data not shown),

but not the over-extension phenotype. It is worth noting the observations of Edwards and Hammarlund that their integrated transgene, in the same chromosomal location, rescued developmental aspects associated with the loss of *sdn-1,* but not the defective axon regenerative phenotype of the DD/VD neurons (Edwards and Hammarlund, 2014). Our subsequent analyses suggested the over-extension phenotype were likely due to over-expression of SDN-1 from the integrated transgenes. Why that specific phenotype might be more acutely sensitive to the amount of SDN-1 being made is not entirely clear, but one hypothesis is that it reflects the fact that axon growth is dynamic during development.

We found no evidence that SDN-1 expressed from the integrated transgenes was expressed in the D-type neurons, despite previous reports that the gene is expressed there (Rhiner et al., 2005). It is certainly possible that the levels of expression are below detection, or that is delayed relative to when we conducted our analyses. However, we did find that we could rescue the over-extension by D-type cell-specific expression. Thus we concluded that, for reasons that are not yet understood, two, separately developed SDN-1 MosSCI inserted transgenes, were not being expressed in the D-type neurons.

SDN-1 functions with EGL-20 to regulate axon termination

Our *sdn-1* rescue experiments did confirm that both the under- and over-growth phenotypes were due to loss of function in *sdn-1.* Further, the cell-specific expression of *sdn-1* suggests a model whereby SDN-1 is acting outside the D-type neurons to facilitate growth from the commissural branch point to the normal termination point. In animals lacking both *sdn-1* and *egl-20* we found fewer animals with under-extended axons, suggesting that SDN-1 was negatively regulating EGL-20 during the initial axon

outgrowth. This is consistent with our evidence and previous reports that EGL-20 primarily functions to inhibit axon outgrowth. Support for this hypothesis came from our observation that we could induce premature axon termination by over-expressing EGL-20, and that we could exacerbate the effects of EGL-20 over-expression by removing SDN-1, consistent with an antagonistic role for SDN-1 in this event. Finally, over-expression of SDN-1 resulted in an *egl-20*-like phenotype of over-extended axons in the DNC.

HS modifications regulate the activity of EGL-20

SDN-1 is the most prominent HSPG in *C. elegans* as detected by an antibody that recognizes the stubs of HS side chains resulting from heparitinase treatment (Hudson et al., 2006). We found that enzymes that modify the heparan sulfate side chains, partially recapitulated the loss of function in *sdn-1,* but likely represent the loss of HS-chains on multiple core proteins, as *sdn-1* and *hse-5* double mutants had an additive effect. Like the loss of *sdn-1*, removing *egl-20* from animals with mutations in the modifier enzymes resulted in fewer under-extended DNCs, consistent with an apparent increase in EGL-20 activity when animals had deficits in HS-modification. Our results are consistent with the modifications being important in mediating proteoglycan interactions with EGL-20. Interestingly, EGL-20 has a poly-basic region (AA288-303 RKATKRLRRKERTERK) that is absent from the posteriorly expressed Wnt ligands LIN-44 and MOM-2. Thus, it is conceivable that EGL-20 interactions are electrostatically favorable with proteins that have been modified with acidic-HS side chains, although this would require a more thorough analysis and remains hypothetical at this point.

Wnt ligands antagonize but BAR-1 and EGL-5 promote posterior axon outgrowth

In canonical Wnt signaling the Wnt ligand results in increased β-catenin activity. Here, although *egl-20* appears to inhibit axon outgrowth, we find that *bar-1/* β-catenin promotes it. Mutations in the Wnt signaling pathway, including *lin-17/frizzled* and *mig-5/disheveled* caused both over-growth and under-growth phenotypes. Interestingly, in all of these mutants we find that D-type axon outgrowth, until the formation of the anterior branch of the dorsal nerve cord, is largely normal. The different effects of mutations in Wnt signaling genes is summarized in Figure 9.

In the *bar-1* mutants however, the posterior branch of the axon in the dorsal cord is almost entirely absent. This suggests that perhaps, *bar-1* is required for the earliest events of axon outgrowth in the posterior branch, although how that would be differentially regulated from the formation of the anterior branch is curious. Ultimately, our results are consistent with previous work demonstrating that *bar-1* acts as a switch for axon growth. When *bar-1* is absent axons are shortened, and when *bar-1* degradation is inhibited axons are overgrown (Maro et al., 2009).

Overall our results suggested that Wnt ligands were not functioning to activate BAR-1 signaling, rather, it appears to be the opposite. In the PLM neurons, recent work has demonstrated that Dishevelled proteins likely regulate the repellant activities of Wnt signaling, by modulating the phosphorylation state of Frizzleds (Zheng et al., 2015). While excitingly similar to our results, there are several differences between the activity of the Wnt ligands and signaling pathway genes on the PLMs and the D-type neurons. Most critically for this point is that the action of *bar-1* was disparate, having only a modest effect on the PLM neurons, but a strong effect on GABAergic outgrowth.

Thus, it is not yet clear how BAR-1 is activated in the D-type neurons to promote axon outgrowth, nor how Wnt signaling is inhibiting BAR-1 signaling in these neurons. Interestingly, *rpm-1* and *anc-1* also appear to function in neurons to potentiate *bar-1* signaling (Tulgren et al., 2014). Thus, it is possible that, some amount of Wnt ligand activity initiates BAR-1 signaling, and this can support axonal development due to the function of RPM-1 and ANC-1.

In the D-type neurons BAR-1 appeared to be necessary to activate the expression of EGL-5, and loss of *egl-5* activity recapitulates the *bar-1* mutant phenotype. Other aspects of D-type neuron morphology are largely intact in the *bar-1* and *egl-5* mutants. For example, the axons extend anterior, they form dorsal commissures properly, *etc.,* it seems most obviously, the posterior branch of the dorsal axon is not formed correctly. From this we propose that EGL-5 is responsible for the transcription of proteins that drive posterior outgrowth. This has been found to be true in other Hox genes, including *mab-5*, which is both necessary and sufficient for the posterior growth of the Q neuroblast descendants (Tamayo et al., 2013).

Wnt-dependent mechanism of axon termination

The wire-minimization hypothesis suggests that axon pathfinding has evolved to provide a balance between the length of process, which reduce neuronal efficiency, and the necessary routing (Stevens, 2012). As a consequence, it is likely that organisms evolved multiple, redundant signals to regulate aspects of pathfinding, including where axons will choose to terminate. Wnt signaling is a primary force in the anterior-posterior guidance of neurons across the animal kingdom (Fenstermaker et al., 2010; Zou, 2004). Here we have found that multiple Wnt ligands collaborate with the syndecan HSPG to regulate

the termination of D-type neurons in a stereotyped position. Although these molecules demonstrate a somewhat complicated pattern of genetic interactions, our results are consistent with them being necessary to reproduce the stereotyped termination of the GABAergic motorneurons in the dorsal nerve cord.

Acknowledgements

We would like to thank Katsu Dejima and Andrew Chisholm for sharing the *juSi119* MosSCI insertion prior to publication. We would also like to thank Vi Leitenberger, Erik Lundquist and Michael Branden for useful discussion and technical support during this work. This work was supported by awards from the NIH (P20GM103418 and P20GM103638).

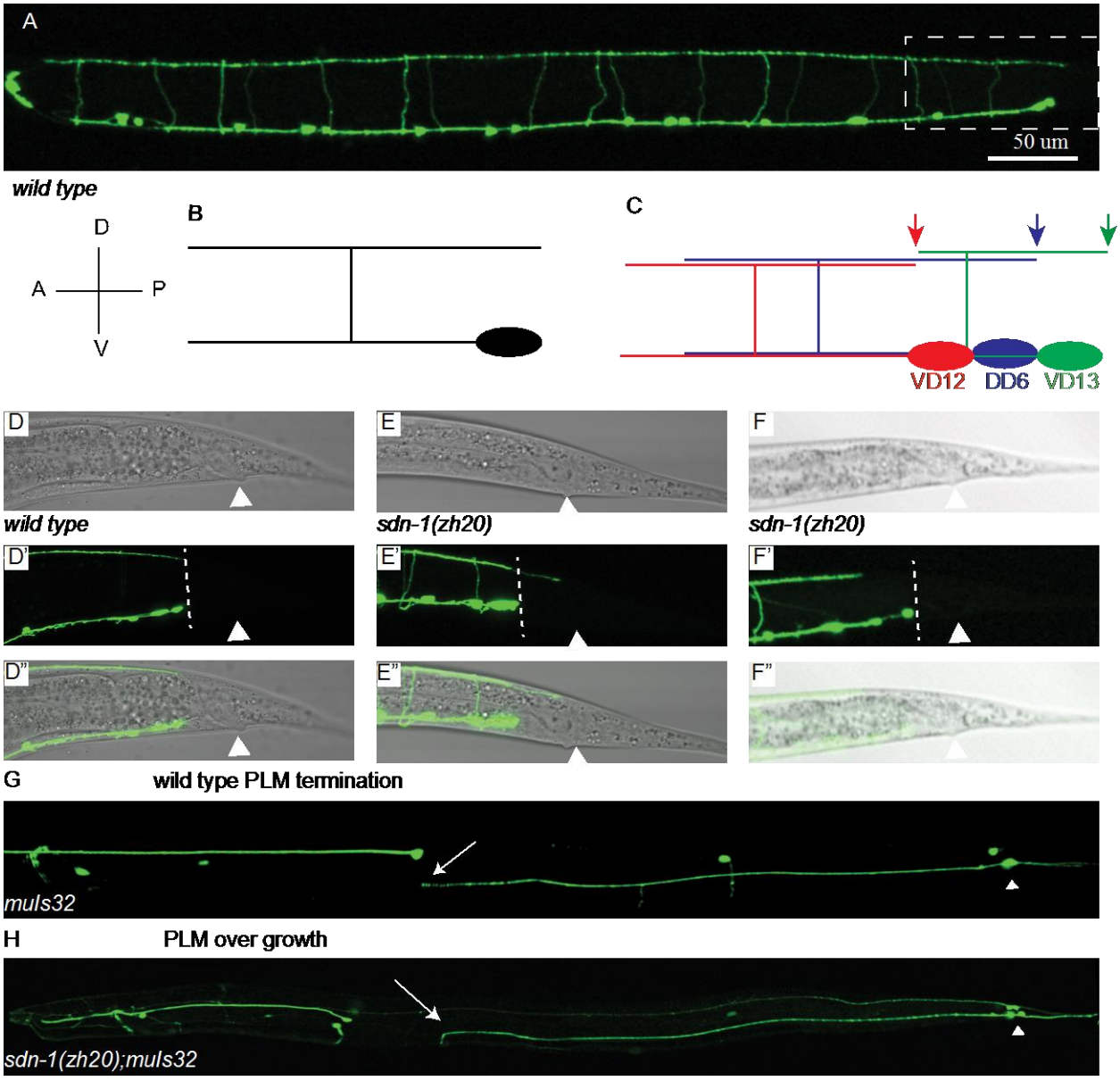

Figure 1 – *sdn-1* regulates VD13 termination in the DNC

A) In an L4 wild-type *juIs76* [*Punc-25::gfp*] animal it is possible to visualize the pattern of axon growth of the GABAergic motorneurons, anterior is left and ventral down in all images. Boxed region in (A) is the tail region equivalent to those presented in (D-F). B) A schematic of the expected morphology of a generic D-type or V-type GABAergic motorneuron, the posterior branch of the dorsal projection terminates approximately at the posterior edge of the cell body. C) A schematic of the terminal three neurons, VD12, DD6 and VD13 and approximate termination points are indicated by arrows. D) A wild type L4 animal where the dorsal nerve cord terminates in a line with the cell bodies (dashed line). The arrowhead indicates the position of the anus. E) An *sdn-1(zh20)* L4 animal with an over-extended DNC, progressed past the plane of the last cell body, and is approximately at the position of the anus. F) An *sdn-1(zh20)* L4 animal with an under-extended DNC, terminating at approximately the position of the DD6 cell body. In wild-type *muIs32* animals the PLM (arrowhead indicates PLM cell body) axons terminate (arrow) along the anterior-posterior axis around the position of the ALM soma. B) In *sdn-1(zh20)* mutants we find that some PLM axons reach the normal termination point and then turn ventrally to continue growth, over-extending. C) Loss of function in *lin-44*/Wnt can result in PLM axons that grow posteriorly and then turn anteriorly, making the PLM appear reversed. D) *lin-44* mutants can also display PLMs were the anterior branch and posterior branch are of approximately equal length. E) The number of animals presenting with each type of PLM growth defect.

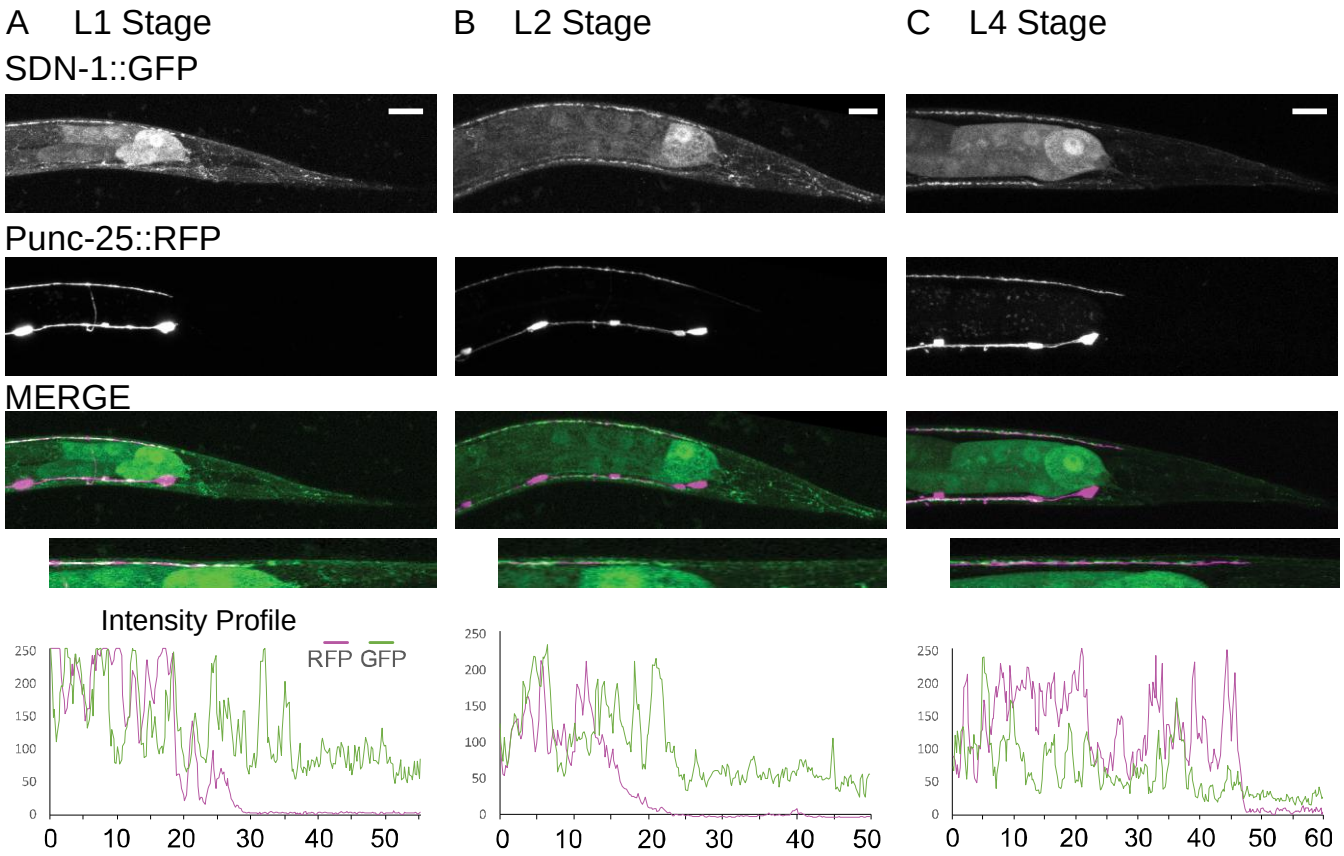

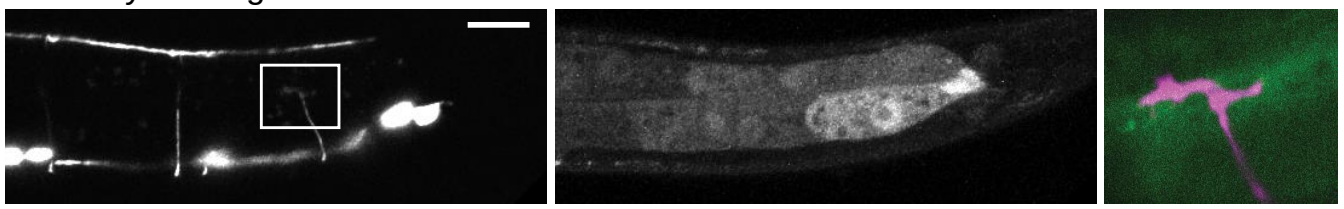

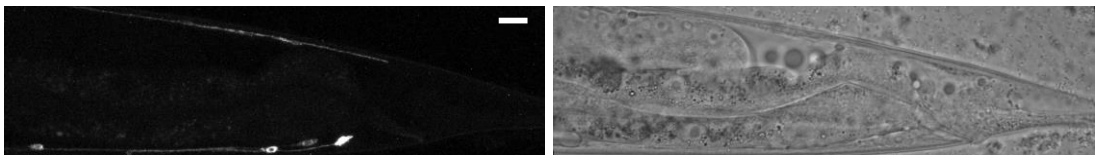

Figure 2 – SDN-1::GFP accumulates near the D-type termination point in the dorsal nerve cord

SDN-1::GFP expression (*juSi119*) relative to the D-type neurons (Punc-25::*rfp*). A) In wild-type first larval stage animals (L1) we find GFP is present in multiple tissues in the tail of the animal and is localized to the dorsal nerve cord. There is an accumulation of SDN-1::GFP near the termination point of the DNC, and this is quantified in the line scan below. No significant differences in the accumulation of SDN-1 were observed as the animals aged through the L2 (B) and L4 (C) larval stages. D) We specifically analyzed SDN-1GFP relative to the *Punc-25*::RFP marker during VD13 outgrowth, but did not observe any obvious accumulation of SDN-1 in the growth cone. E) Expression of an SDN-1::GFP chimera specifically in the D-type neurons. SDN-1 localized primarily to the dorsal and ventral nerve cords, and was present near the expected termination of the D-type neurons (arrowhead).

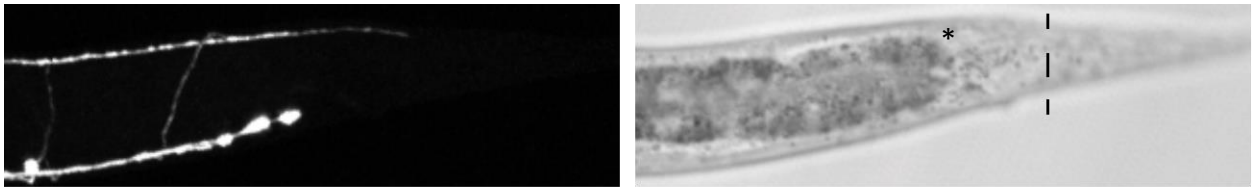

lin-44(n1792)

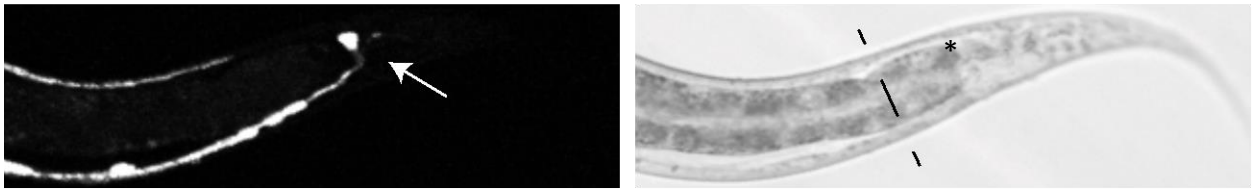

lin-44(n1792);sdn-1(zh20)

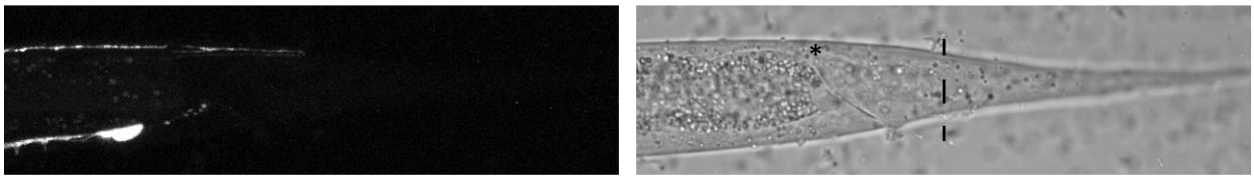

lin-44(n1792);sdn-1(zh20)

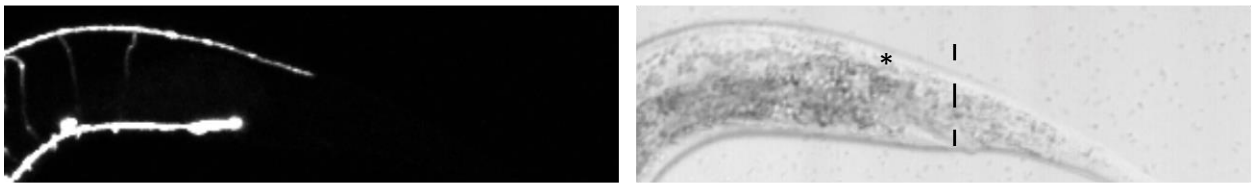

egl-20(gk453010)

Figure 3 – *lin-44* and *egl-20* Wnt ligands regulate the termination point of the dorsal nerve cord

Loss of function mutations in *lin-44* result in the DNC overextending into the posterior regions of the animal. The arrowhead indicates the expected termination point. In the DIC image the dashed line indicates the termination point of the axon fascicle in the animal. The asterisks indicate the approximate wild-type termination point. Note, the *lin-44; zh20* animals were visualized using *oxIs12* which also labels the DVB neuron (arrow), which is located just posterior and slightly dorsal to the VD13 cell body.

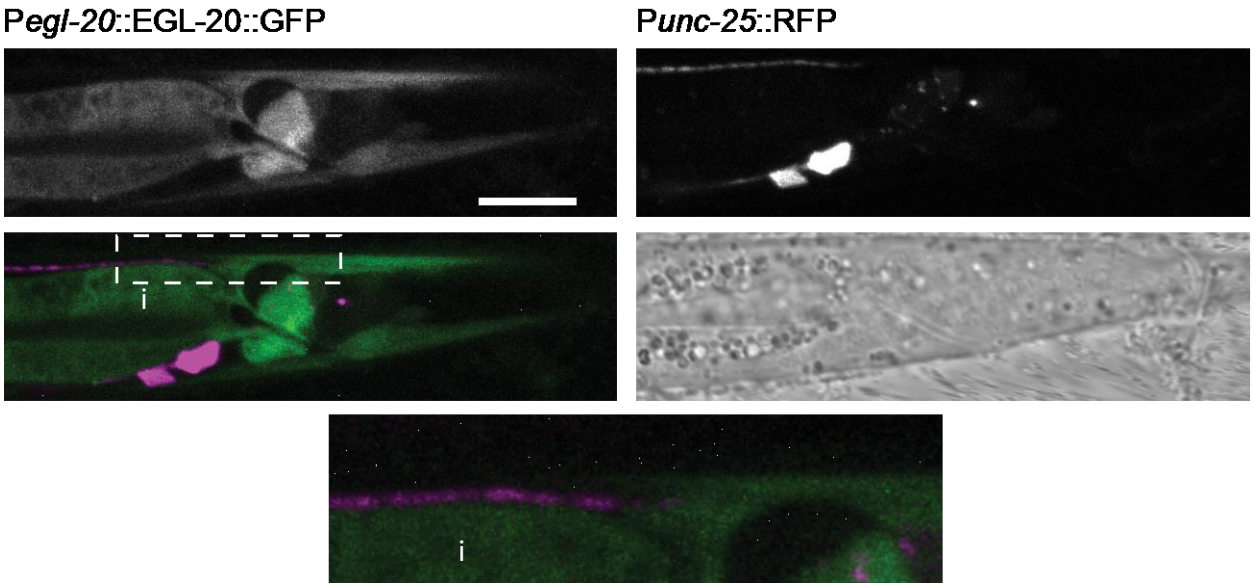

Figure 4 – The GABAergic neurons termination is coordinate with EGL-20 localization

We examined the localization of EGL-20::GFP relative to the termination point of the GABAergic neurons in L2 animals. We found that the axons frequently terminate in regions where EGL-20 accumulates. Note the GFP in the intestine (i) is an artifact of the co-injection marker, and is intracellular.

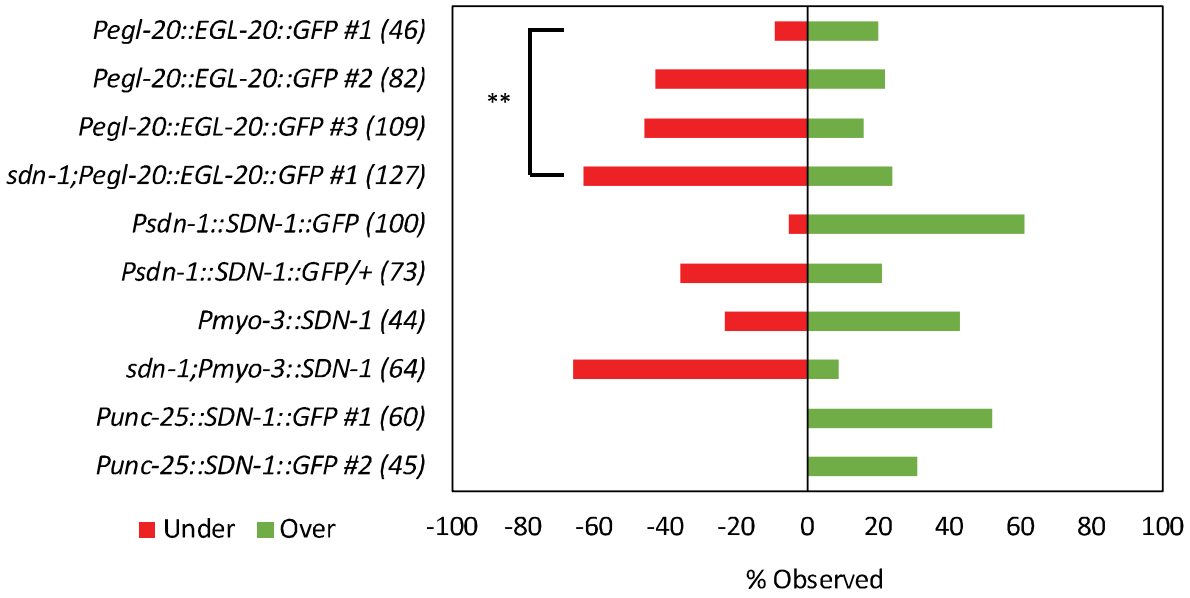

Figure 5 – EGL-20 induces axon termination dependent on SDN-1

Overexpression of the EGL-20 transgene induced premature termination, while SDN-1 over-expression was associated with over-extension defects. Removing *sdn-1* from animals over-expressing EGL-20 increased the penetrance of premature termination defects. Cell-specifically over-expressing *sdn-1* in the GABAergic neurons resulted in over-extension defects. These results suggest that SDN-1 and EGL-20 acted antagonistically in axon termination.

L2 - wild type

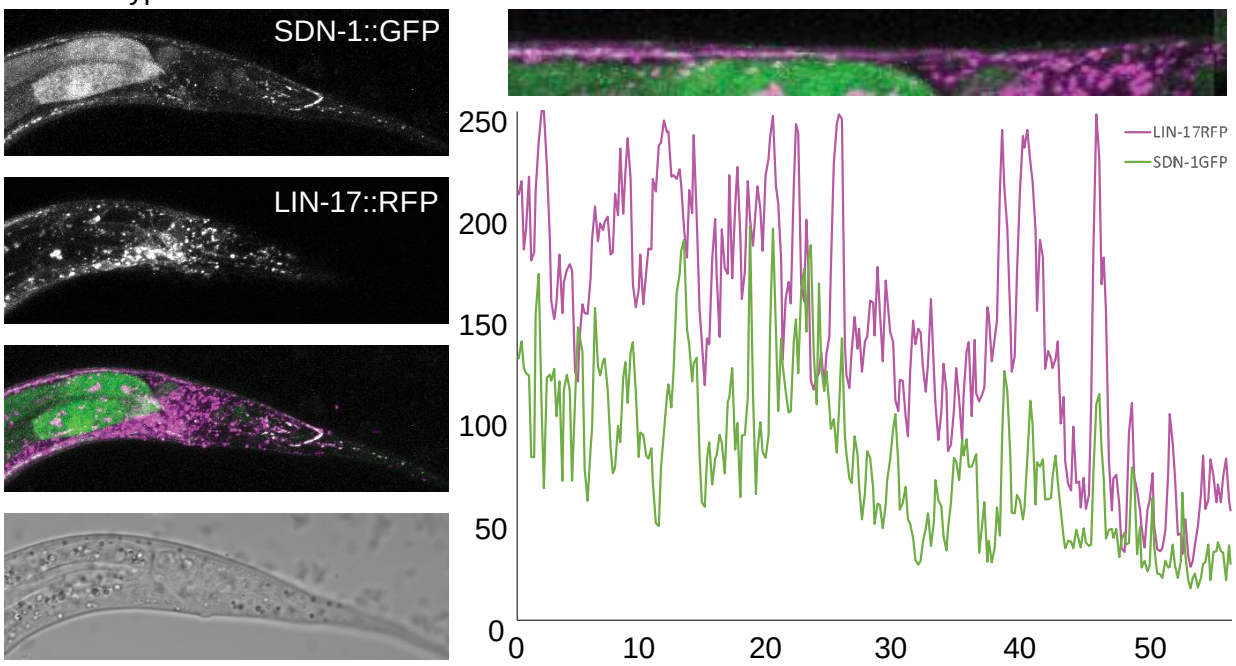

L2 - *egl-20(gk453010)*

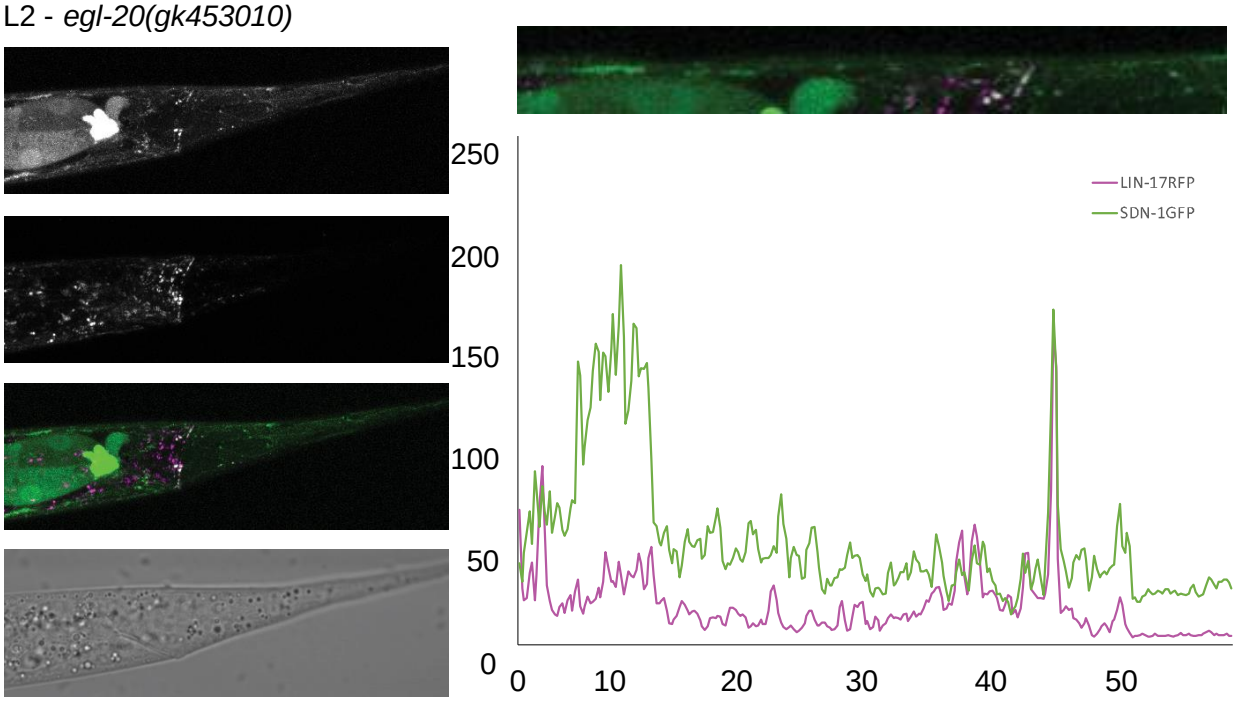

Figure 6 – SDN-1 and LIN-17 co-localize to the dorsal nerve cord in an *egl-20*-dependent manner

Loss of function in *sdn-1* and *lin-17* had equal effects on axon outgrowth, and the proteins appear to co-localize in the dorsal nerve cord in L2 animals. Conversely, in *egl-20* loss of function animals while SDN-1::GFP localization is largely similar to wild-type, LIN-17::RFP accumulation was reduced, especially within the dorsal nerve cord.

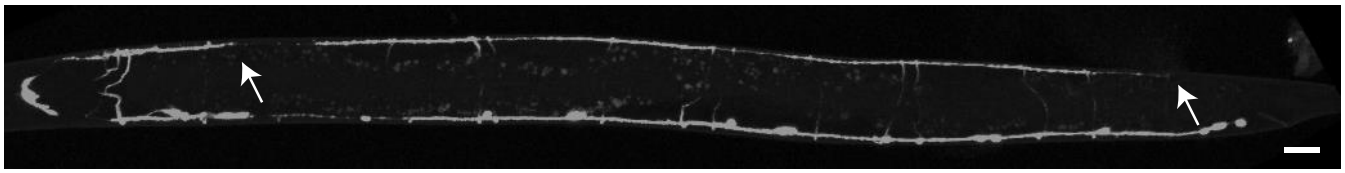

bar-1(ga80)

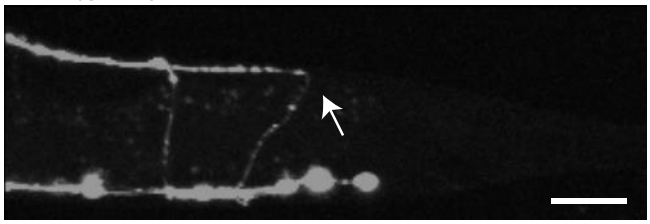

bar-1(ga80)

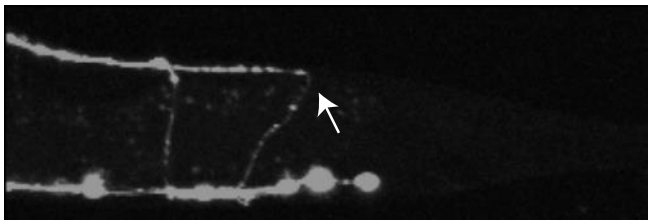

bar-1; egl-20

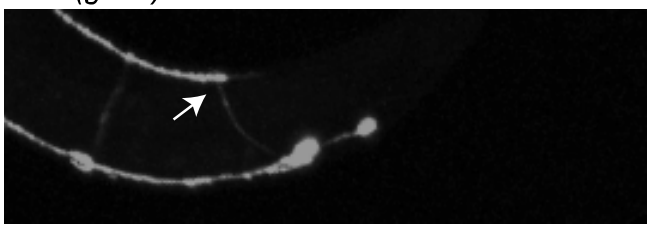

egl-5(n945)

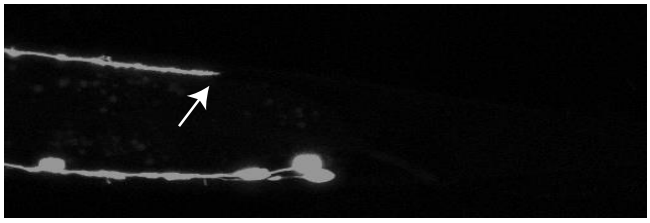

egl-5; sdn-1

Figure 7 – Axon underextension in *bar-1* and *egl-5* mutants

The D-type neurons in *bar-1* mutants exhibit premature termination (arrows). Specifically, in the tail, most frequently the posterior branch of the dorsal axon fails to form or is shortened. *egl-5* mutants have a similar phenotype, with a axon that grows only a short distance from the commissural branch point.

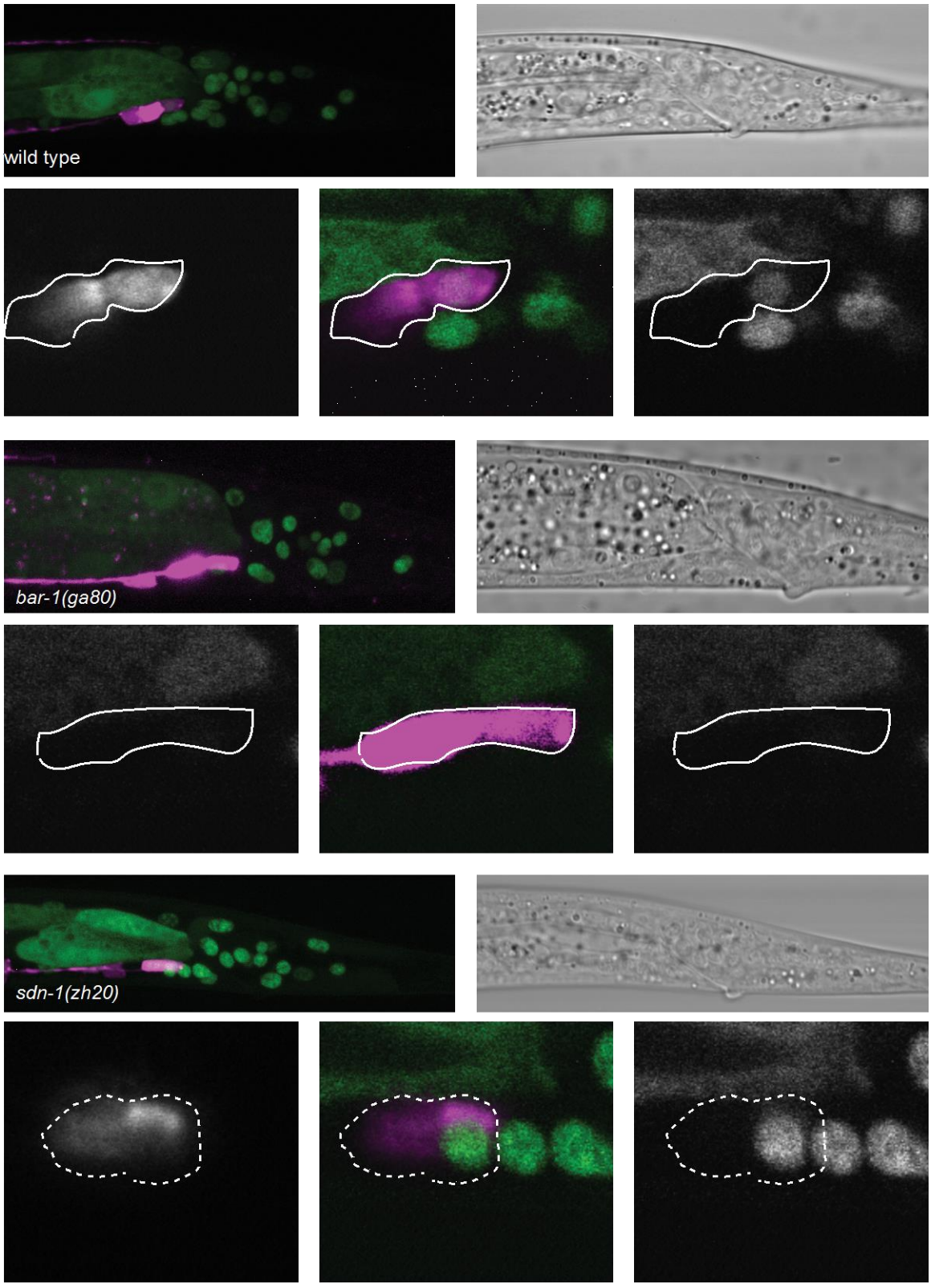

Figure 8 – EGL-5GFP is expressed in the GABAergic motorneurons in a *bar-1*-dependent manner

We examined the expression of EGL-5 using a P*egl-5::*EGL-5::GFP transgene that rescued the mutant defects associated with the (*n945*) phenotype. EGL-5::GFP was transiently expressed in the most posterior D-type neurons, along with other cells in the tail. Loss-of-function in *bar-1* results in a complete loss of EGL-5 expression in the D-type neurons, and some other cells in the tail, although not a complete loss of EGL-5 expression altogether. The effect of *sdn-1* loss-of-function was more variable, but expression was not eliminated from the D-type neurons.

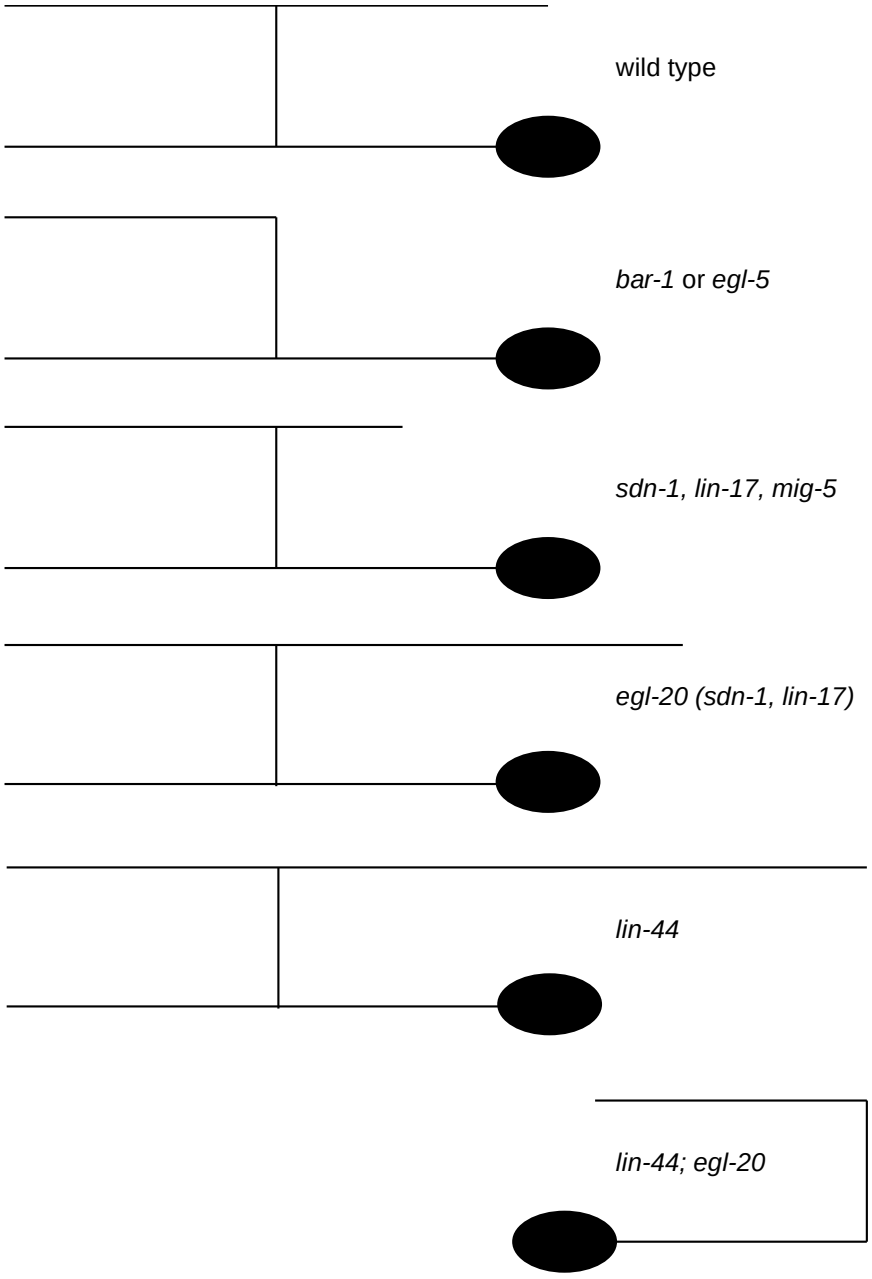

Figure 9 – Axon extension by genotype

The different neuronal morphologies observed most commonly in the different mutant backgrounds. In wild type the D-type neurons have an "H" shape with roughly equal anterior and posterior branches in the dorsal cord. The *bar-1* and *egl-5* mutants are frequently missing or have very short posterior branches with largely intact anterior branches. The *sdn-1, lin-17* and *mig-5* mutants have formed, but shortened posterior branches, while the *egl-20,* and occasionally *sdn-1* and *lin-17*, mutants have longer than expected posterior branches. The *lin-44* mutants have axons that project further posterior than in the other genetic backgrounds. Finally, several of the mutants have posterior neurites, where the axon appears to project toward the posterior of the animal, instead of the anterior. These were highly prevalent in the *lin-44; egl-20* double mutants.

PLM reversed

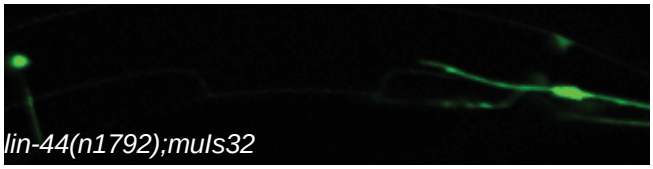

PLM equal

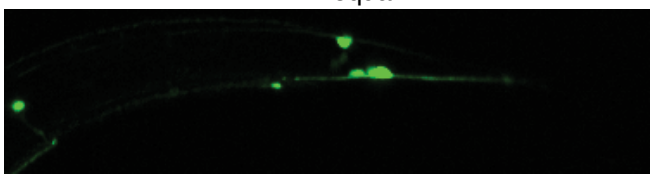

Supplementary Figure 1 – PLM defects in *lin-44* mutants

PLM neurons in *lin-44* mutants could be observed to have reversed morphologies, where the posterior branch of the axon is much longer than the anterior branch. The axon projected into the tail and then turn anterior projecting past the cell body. In other animals the anterior and posterior branches exhibit approximately equal lengths.

Literature Cited

Alexander, C.M., F. Reichsman, M.T. Hinkes, J. Lincecum, K.A. Becker, S. Cumberledge, and M. Bernfield. 2000. Syndecan-1 is required for Wnt-1-induced mammary tumorigenesis in mice. *Nat Genet*. 25:329-332.

Aricescu, A.R., I.W. McKinnell, W. Halfter, and A.W. Stoker. 2002. Heparan sulfate proteoglycans are ligands for receptor protein tyrosine phosphatase sigma. *Mol Cell Biol*. 22:1881-1892.

Baeg, G.H., and N. Perrimon. 2000. Functional binding of secreted molecules to heparan sulfate proteoglycans in Drosophila. *Curr Opin Cell Biol*. 12:575-580.

Bernfield, M., R. Kokenyesi, M. Kato, M.T. Hinkes, J. Spring, R.L. Gallo, and E.J. Lose. 1992. Biology of the syndecans: a family of transmembrane heparan sulfate proteoglycans. *Annu Rev Cell Biol*. 8:365-393.

Bishop, J.R., M. Schuksz, and J.D. Esko. 2007. Heparan sulphate proteoglycans fine-tune mammalian physiology. *Nature*. 446:1030-1037.

Brenner, S. 1974. The genetics of Caenorhabditis elegans. *Genetics*. 77:71-94.

Buechling, T., and M. Boutros. 2011. Wnt signaling signaling at and above the receptor level. *Curr Top Dev Biol*. 97:21-53.

Bulow, H.E., and O. Hobert. 2004. Differential sulfations and epimerization define heparan sulfate specificity in nervous system development. *Neuron*. 41:723-736.

Bulow, H.E., N. Tjoe, R.A. Townley, D. Didiano, T.H. van Kuppevelt, and O. Hobert. 2008. Extracellular sugar modifications provide instructive and cell-specific information for axon-guidance choices. *Curr Biol*. 18:1978-1985.

Cohen, A.R., D.F. Woods, S.M. Marfatia, Z. Walther, A.H. Chishti, and J.M. Anderson. 1998. Human CASK/LIN-2 binds syndecan-2 and protein 4.1 and localizes to the basolateral membrane of epithelial cells. *J Cell Biol*. 142:129-138.

Dejima, K., S. Kang, S. Mitani, P.C. Cosman, and A.D. Chisholm. 2014. Syndecan defines precise spindle orientation by modulating Wnt signaling in C. elegans. *Development*. 141:4354-4365.

Diaz-Balzac, C.A., M.I. Lazaro-Pena, E. Tecle, N. Gomez, and H.E. Bulow. 2014. Complex cooperative functions of heparan sulfate proteoglycans shape nervous system development in Caenorhabditis elegans. *G3*. 4:1859-1870.

Edwards, T.J., and M. Hammarlund. 2014. Syndecan promotes axon regeneration by stabilizing growth cone migration. *Cell reports*. 8:272-283.

Fenstermaker, A.G., A.A. Prasad, A. Bechara, Y. Adolfs, F. Tissir, A. Goffinet, Y. Zou, and R.J. Pasterkamp. 2010. Wnt/planar cell polarity signaling controls the anterior-posterior organization of monoaminergic axons in the brainstem. *J Neurosci*. 30:16053-16064.

Forrester, W.C., M. Dell, E. Perens, and G. Garriga. 1999. A C. elegans Ror receptor tyrosine kinase regulates cell motility and asymmetric cell division. *Nature*. 400:881-885.

Forrester, W.C., C. Kim, and G. Garriga. 2004. The Caenorhabditis elegans Ror RTK CAM-1 inhibits EGL-20/Wnt signaling in cell migration. *Genetics*. 168:1951-1962.

Green, J.L., T. Inoue, and P.W. Sternberg. 2007. The C. elegans ROR receptor tyrosine kinase, CAM-1, non-autonomously inhibits the Wnt pathway. *Development*. 134:4053-4062.

Grill, B., W.V. Bienvenut, H.M. Brown, B.D. Ackley, M. Quadroni, and Y. Jin. 2007. C. elegans RPM-1 regulates axon termination and synaptogenesis through the Rab GEF GLO-4 and the Rab GTPase GLO-1. *Neuron*. 55:587-601.

Harterink, M., D.H. Kim, T.C. Middelkoop, T.D. Doan, A. van Oudenaarden, and H.C. Korswagen. 2011. Neuroblast migration along the anteroposterior axis of C. elegans is controlled by opposing gradients of Wnts and a secreted Frizzled-related protein. *Development*. 138:2915-2924.

Hartin, S.N., M.L. Hudson, C. Yingling, and B.D. Ackley. 2015. A synthetic lethal screen identifies a role for lin-44/Wnt in C. elegans embryogenesis. *PLoS One*. In Press.

Hayashi, Y., T. Hirotsu, R. Iwata, E. Kage-Nakadai, H. Kunitomo, T. Ishihara, Y. Iino, and T. Kubo. 2009. A trophic role for Wnt-Ror kinase signaling during developmental pruning in Caenorhabditis elegans. *Nat Neurosci*. 12:981-987.

Hilliard, M.A., and C.I. Bargmann. 2006. Wnt signals and frizzled activity orient anterior-posterior axon outgrowth in C. elegans. *Dev Cell*. 10:379-390.

Hobert, O., K. Tessmar, and G. Ruvkun. 1999. The Caenorhabditis elegans lim-6 LIM homeobox gene regulates neurite outgrowth and function of particular GABAergic neurons. *Development*. 126:1547-1562.

Hsueh, Y.P., and M. Sheng. 1999. Regulated expression and subcellular localization of syndecan heparan sulfate proteoglycans and the syndecan-binding protein CASK/LIN-2 during rat brain development. *J Neurosci*. 19:7415-7425.

Huang, X., H.J. Cheng, M. Tessier-Lavigne, and Y. Jin. 2002. MAX-1, a novel PH/MyTH4/FERM domain cytoplasmic protein implicated in netrin-mediated axon repulsion. *Neuron*. 34:563-576.

Huang, X., P. Huang, M.K. Robinson, M.J. Stern, and Y. Jin. 2003. UNC-71, a disintegrin and metalloprotease (ADAM) protein, regulates motor axon guidance and sex myoblast migration in C. elegans. *Development*. 130:3147-3161.

Huarcaya Najarro, E., and B.D. Ackley. 2013. C. elegans fmi-1/flamingo and Wnt pathway components interact genetically to control the anteroposterior neurite growth of the VD GABAergic neurons. *Dev Biol*. 377:224-235.

Hudson, M.L., T. Kinnunen, H.N. Cinar, and A.D. Chisholm. 2006. C. elegans Kallmann syndrome protein KAL-1 interacts with syndecan and glypican to regulate neuronal cell migrations. *Dev Biol*. 294:352-365.

Inatani, M., F. Irie, A.S. Plump, M. Tessier-Lavigne, and Y. Yamaguchi. 2003. Mammalian brain morphogenesis and midline axon guidance require heparan sulfate. *Science*. 302:1044-1046.

Kennerdell, J.R., R.D. Fetter, and C.I. Bargmann. 2009. Wnt-Ror signaling to SIA and SIB neurons directs anterior axon guidance and nerve ring placement in C. elegans. *Development*. 136:3801-3810.

Lee, J.S., and C.B. Chien. 2004. When sugars guide axons: insights from heparan sulphate proteoglycan mutants. *Nat Rev Genet*. 5:923-935.

Maro, G.S., M.P. Klassen, and K. Shen. 2009. A beta-catenin-dependent Wnt pathway mediates anteroposterior axon guidance in C. elegans motor neurons. *PLoS ONE*. 4:e4690.

Minami, Y., I. Oishi, M. Endo, and M. Nishita. 2010. Ror-family receptor tyrosine kinases in noncanonical Wnt signaling: their implications in developmental morphogenesis and human diseases. *Dev Dyn*. 239:1-15.

Minniti, A.N., M. Labarca, C. Hurtado, and E. Brandan. 2004. Caenorhabditis elegans syndecan (SDN-1) is required for normal egg laying and associates with the nervous system and the vulva. *J Cell Sci*. 117:5179-5190.

Niu, W., Z.J. Lu, M. Zhong, M. Sarov, J.I. Murray, C.M. Brdlik, J. Janette, C. Chen, P. Alves, E. Preston, C. Slightham, L. Jiang, A.A. Hyman, S.K. Kim, R.H. Waterston, M. Gerstein, M. Snyder, and V. Reinke. 2011. Diverse transcription factor binding features revealed by genome-wide ChIP-seq in C. elegans. *Genome Res*. 21:245-254.

Norris, A.D., and E.A. Lundquist. 2011. UNC-6/netrin and its receptors UNC-5 and UNC-40/DCC modulate growth cone protrusion in vivo in C. elegans. *Development*. 138:4433-4442.

Ohama, Y., and K. Hayashi. 2009. Relocalization of a microtubule-anchoring protein, ninein, from the centrosome to dendrites during differentiation of mouse neurons. *Histochem Cell Biol*. 132:515-524.

Opperman, K.J., and B. Grill. 2014. RPM-1 is localized to distinct subcellular compartments and regulates axon length in GABAergic motor neurons. *Neural Dev*. 9:10.

Rawson, J.M., B. Dimitroff, K.G. Johnson, X. Ge, D. Van Vactor, and S.B. Selleck. 2005. The heparan sulfate proteoglycans Dally-like and Syndecan have distinct functions in axon guidance and visual-system assembly in Drosophila. *Curr Biol*. 15:833-838.

Rhiner, C., S. Gysi, E. Frohli, M.O. Hengartner, and A. Hajnal. 2005. Syndecan regulates cell migration and axon guidance in C. elegans. *Development*. 132:4621-4633.

Schwabiuk, M., L. Coudiere, and D.C. Merz. 2009. SDN-1/syndecan regulates growth factor signaling in distal tip cell migrations in C. elegans. *Dev Biol*. 334:235-242.

Schwieterman, A.A., A.N. Steves, V. Yee, C.J. Donelson, M.R. Bentley, E.M. Santorella, T.V. Mehlenbacher, A. Pital, A.M. Howard, M.R. Wilson, D.E. Ereddia, K.S. Effrein, J.L. McMurry, B.D. Ackley, A.D. Chisholm, and M.L. Hudson. 2016. The Caenorhabditis elegans Ephrin EFN-4 Functions Non-cell Autonomously with Heparan Sulfate Proteoglycans to Promote Axon Outgrowth and Branching. *Genetics*. 202:639-660.

Shen, Y. 2014. Traffic lights for axon growth: proteoglycans and their neuronal receptors. *Neural regeneration research*. 9:356-361.

Song, S., B. Zhang, H. Sun, X. Li, Y. Xiang, Z. Liu, X. Huang, and M. Ding. 2010. A Wnt-Frz/Ror-Dsh pathway regulates neurite outgrowth in Caenorhabditis elegans. *PLoS Genet*. 6.

Steigemann, P., A. Molitor, S. Fellert, H. Jackle, and G. Vorbruggen. 2004. Heparan sulfate proteoglycan syndecan promotes axonal and myotube guidance by slit/robo signaling. *Curr Biol*. 14:225-230.

Stevens, C.F. 2012. Brain organization: wiring economy works for the large and small. *Curr Biol*. 22:R24-25.

Tamayo, J.V., M. Gujar, S.J. Macdonald, and E.A. Lundquist. 2013. Functional transcriptomic analysis of the role of MAB-5/Hox in Q neuroblast migration in Caenorhabditis elegans. *BMC Genomics*. 14:304.

Thompson, O., M. Edgley, P. Strasbourger, S. Flibotte, B. Ewing, R. Adair, V. Au, I. Chaudhry, L. Fernando, H. Hutter, A. Kieffer, J. Lau, N. Lee, A. Miller, G. Raymant, B. Shen, J. Shendure, J. Taylor, E.H. Turner, L.W. Hillier, D.G. Moerman, and R.H. Waterston. 2013. The million mutation project: a new approach to genetics in Caenorhabditis elegans. *Genome Res*. 23:1749-1762.

Tulgren, E.D., S.M. Turgeon, K.J. Opperman, and B. Grill. 2014. The Nesprin family member ANC-1 regulates synapse formation and axon termination by functioning in a pathway with RPM-1 and beta-Catenin. *PLoS Genet*. 10:e1004481.

Tumova, S., A. Woods, and J.R. Couchman. 2000. Heparan sulfate proteoglycans on the cell surface: versatile coordinators of cellular functions. *Int J Biochem Cell Biol*. 32:269-288.

Wang, X., J. Liu, Z. Zhu, and G. Ou. 2015. The heparan sulfate-modifying enzyme glucuronyl C5-epimerase HSE-5 controls Caenorhabditis elegans Q neuroblast polarization during migration. *Dev Biol*. 399:306-314.

White, J.G., E. Southgate, J.N. Thomson, and S. Brenner. 1986. The structure of the nervous system of the nematode Caenorhabditis elegans. *Philos Trans R Soc Lond B Biol Sci*. 314:1-340.

Wightman, B., R. Baran, and G. Garriga. 1997. Genes that guide growth cones along the C. elegans ventral nerve cord. *Development*. 124:2571-2580.

Yamaguchi, Y. 2001. Heparan sulfate proteoglycans in the nervous system: their diverse roles in neurogenesis, axon guidance, and synaptogenesis. *Semin Cell Dev Biol*. 12:99-106.

Zheng, C., M. Diaz-Cuadros, and M. Chalfie. 2015. Dishevelled attenuates the repelling activity of Wnt signaling during neurite outgrowth in Caenorhabditis elegans. *Proc Natl Acad Sci U S A*. 112:13243-13248.

Zou, Y. 2004. Wnt signaling in axon guidance. *Trends Neurosci*. 27:528-532.